Bioactive Materials 45 (2025) 274–300

Contents lists available at ScienceDirect

Bioactive Materials

journal homepage: www.keaipublishing.com/en/journals/bioactive-materials

Review article

Microneedle technology for enhanced topical treatment of skin infections

Tingting Peng [a,**], Yangyan Chen [b], Xuanyu Luan [c], Wanshan Hu [a], Wentao Wu [b], Bing Guo [d,***], Chao Lu [a,****], Chuanbin Wu [a], Xin Pan [b,*]

[a] State Key Laboratory of Bioactive Molecules and Druggability Assessment/ International Cooperative Laboratory of Traditional Chinese Medicine Modernization and Innovative Drug Development of Ministry of Education (MOE) of China/College of Pharmacy, Jinan University, Guangzhou 511436, China
[b] School of Pharmaceutical Sciences, Sun Yat-sen University, Guangzhou 510006, China
[c] Department of Metabolism, Digestion and Reproduction, Faculty of Medicine, Imperial College London, London, W12 0NN, UK
[d] School of Science, Harbin Institute of Technology, Shenzhen 518055, China

ARTICLE INFO

Keywords:
Microneedle
Skin infection
Topical treatment
Biosensing
Drug delivery systems

ABSTRACT

Skin infections caused by microbes such as bacteria, fungi, and viruses often lead to aberrant skin functions and appearance, eventually evolving into a significant risk to human health. Among different drug administration paradigms for skin infections, microneedles (MNs) have demonstrated superiority mainly because of their merits in enhancing drug delivery efficiency and reducing microbial resistance. Also, integrating biosensing functionality to MNs offers point-of-care wearable medical devices for analyzing specific pathogens, disease status, and drug pharmacokinetics, thus providing personalized therapy for skin infections. Herein, we do a timely update on the development of MN technology in skin infection management, with a special focus on how to devise MNs for personalized antimicrobial therapy. Notably, the advantages of state-of-the-art MNs for treating skin infections are pointed out, which include hijacking sequential drug transport barriers to enhance drug delivery efficiency and delivering various therapeutics (*e.g.*, antibiotics, antimicrobial peptides, photosensitizers, metals, sonosensitizers, nanoenzyme, living bacteria, poly ionic liquid, and nanomoter). In addition, the nanoenzyme-based multimodal antimicrobial therapy is highlighted in addressing intractable infectious wounds. Furthermore, the MN-based biosensors used to identify pathogen types, track disease status, and quantify antibiotic concentrations are summarized. The limitations of antimicrobial MNs toward clinical translation are offered regarding large-scale production, quality control, and policy guidance. Finally, the future development of biosensing MNs with easy-to-use and intelligent properties and MN-based wearable drug delivery for home-based therapy are prospected. We hope this review will provide valuable guidance for future development in MN-mediated topical treatment of skin infections.

1. Introduction

It is well known that the skin is the largest organ of the human body and plays a vital role in safeguarding the body against the invasion of external pathogens. Skin infections can arise from various external factors such as traumas, burns, scalds, and internal ailments like diabetes and pressure ulcers [1]. Once the structural and functional integrity of the skin is impaired, the microbes, including bacteria, fungi, and viruses, prefer to migrate from the surface of the skin to the subcutaneous tissue. This would lead to various skin infections ranging from mild superficial infections to severe deep soft tissue infections, consuming enormous medical resources. At present, antibiotics is the mainstay for treating skin infections, but it is usually ineffective for intractable skin infections, such as skin soft tissue infections (SSTIs), and chronic wound infections. This is because only a minimal amount of antibiotics can be delivered to the infection site via conventional oral, injectable, or transdermal administration routes [2,3]. Therefore, it is crucial to develop an alternative delivery system with enhanced drug

Peer review under responsibility of KeAi Communications Co., Ltd.
* Corresponding authors.
** Corresponding author. College of Pharmacy, Jinan University, Guangzhou 511436, China.
*** Corresponding authors.
**** Corresponding author. College of Pharmacy, Jinan University, Guangzhou 511436, China.
E-mail addresses: pengtt@jnu.edu.cn (T. Peng), guobing2020@hit.edu.cn (B. Guo), chaolu@jnu.edu.cn (C. Lu), panxin2@mail.sysu.edu.cn (X. Pan).

https://doi.org/10.1016/j.bioactmat.2024.11.027
Received 20 January 2024; Received in revised form 31 October 2024; Accepted 20 November 2024

delivery efficiency for treating skin infections.

Topical treatment of skin infections is effective in improving therapeutic efficacy whilst minimizing adverse effects. However, the delivery efficiency of therapeutics can be largely restricted by several major drug transport barriers, which further compromise antimicrobial effects. Stratum corneum with compact brick-wall structure and tight junction is generally recognized as the foremost barrier against drug permeation across the skin [4]. Cell debris and necrotic tissue constitute unignored subcutaneous barriers that restrict drug transport to infected tissues [5]. In particular, the biofilm defined as a collection of mono-microbial or polymicrobial communities, serves as another rigid barrier that severely hinders the diffusion and penetration of drugs into biofilm, as it comprises highly dense extracellular polymeric substances (EPS) [6]. EPS are primarily composed of polysaccharides, proteins, extracellular DNA (eDNA), and water-insoluble compounds (*e.g.*, lipids, amyloids, cellulose), accounting for more than 90 % of the biofilm mass [7,8]. The biofilm can protect the microbial cells from attack by antibiotics and host's immune defense, and even secrete specific enzymes (*e.g.*, β-lactamases, extended spectrum β-lactamases, and aminoglycoside modifying enzyme) to hydrolyze antibiotics, leading to treatment failure. As a result, the resistance of biofilm to antibiotics is usually 10–1000 times higher than that of planktonic bacteria [9,10]. Therefore, it is crucial to overcome sequential drug barriers for improved antimicrobial efficacy.

Recently, we and other groups have found that microneedles (MNs) are good administration tools for topical treatment of skin infections [11–13]. As shown in Fig. 1a, MNs can pierce the skin in a minimally invasive manner without stimulating dermal nerves and blood vessels, thus exerting no pain on patients [14]. During the process of MNs piercing the skin, skin micropores can be transiently created for the delivery of the therapeutics to the epidermis and upper dermis. In addition, MNs can cause physical damage to the biofilm to increase the penetration of antimicrobials into the biofilm. The introduction of agents that help to damage EPS into MNs can further improve the exposure of the drug to naked microbial cells and antibiofilm effects, such as specific enzymes (*e.g.*, α-amylase [15]), external stimulus (*e.g.*, light [12], ultrasound [16]), and gas nanomotors [17]). Therefore, microneedling technology helps the loaded therapeutics to hijack the multiple transport barriers constituted of stratum corneum, cell debris, necrotic tissue, and biofilms (Fig. 1b). These attributes make MNs have no strict restrictions on the molecular weight (MW < 500 Da), hydrophilicity ($1 < \log(P) < 3$), and melting point of the delivered therapeutic agents. To date, MNs have been increasingly used to deliver a wide range of therapeutics to the infection site for diverse therapies, including small-molecular therapeutic agents (*e.g.*, antibiotics, photosensitizers, sonosensitizers), large-molecular antimicrobials (*e.g.*, antimicrobial peptide, poly ionic liquid), nanometer-sized particles (*e.g.*, nanospheres,

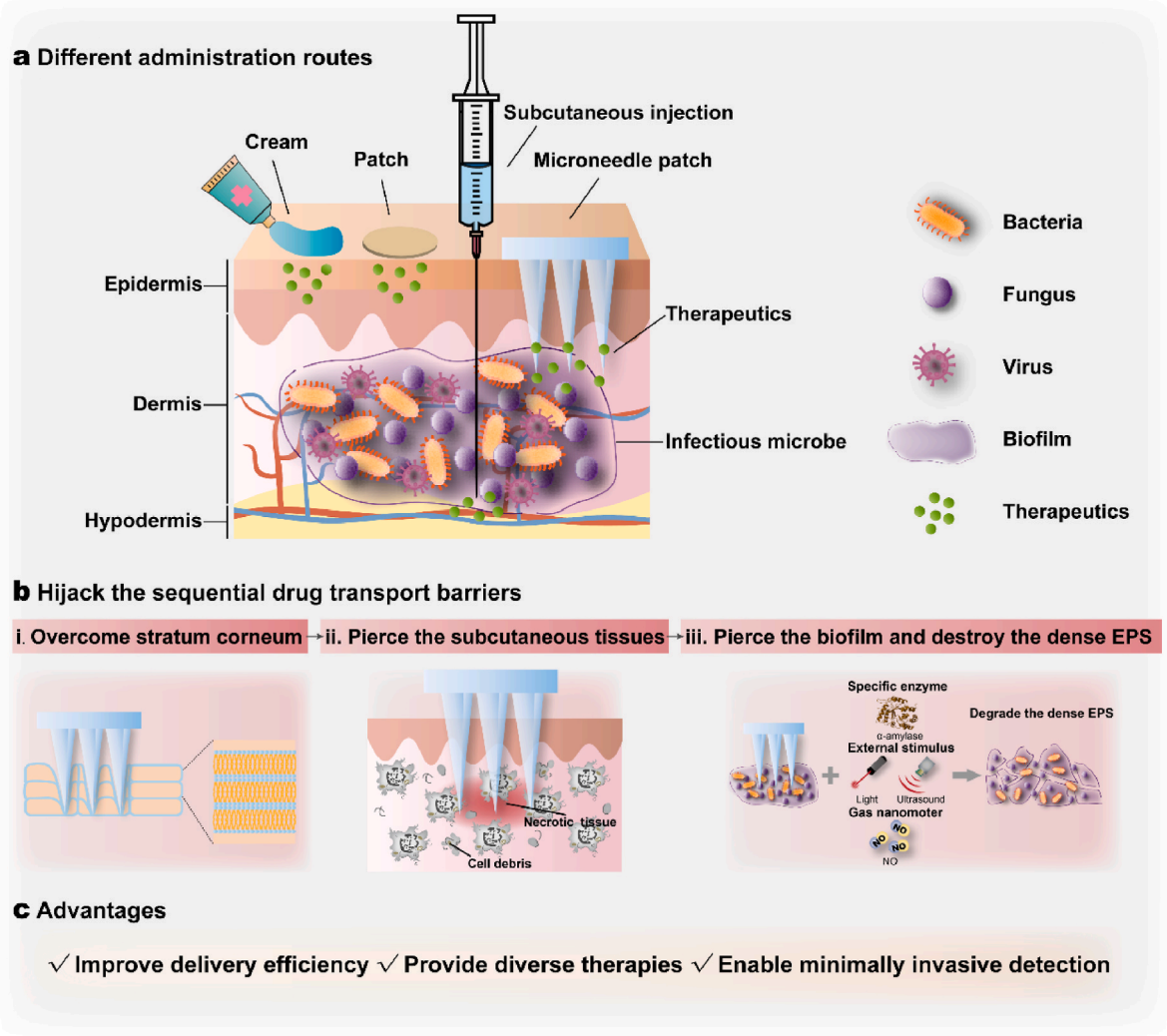

Fig. 1. MNs are promising administration tools for managing skin infections: **(a)** Comparision of different administration routes, including transdermal preparations (*e.g.*, cream, patch), hypodermic injections, and MNs. **(b)** MNs with proper design can hijack the sequential drug delivery barriers involved in skin infections. **(c)** MNs offer distinct advantages in managing skin infections.

nanosheets, nanomoters), and living bacteria [18]. Particularly, the integration of biosensing function to MNs can be constructed as wearable medical devices to provide real-time monitoring of specific pathogens, disease status, and drug pharmacokinetics, which contributes to personalized therapy for skin infections [19–23]. On the whole, MNs offer notable benefits in enhancing drug delivery efficiency, providing diverse therapies, and enabling minimally invasive detection.

Based on the modes of drug loading and delivery, MNs can be classified into five types: (1) solid MNs made of silicon, metals, or polymers, first pierce the skin to create mechanical micropores, and then are removed for the delivery of drug loaded in the patch or cream; (2) hollow MNs, also known as microsyringes, have a cavity inside the needle that can serve as a microchannel for drug injection; (3) coated MNs can be prepared from solid MNs that are coated with drug by dip coating, spray drying, and so on; (4) hydrogel MNs containing polymeric needles that can swell in the skin to create microchannels for the delivery of drug loaded in the baseplate; and (5) dissolving MNs containing drug-loaded needles can directly pierce the skin to release the drug inside. In recent years, various types of MNs have been devised to treat and diagnose skin infections [24–26].

We herein offer a timely and comprehensive summary of MN-mediated diverse antimicrobial therapies, MN-based biosensors, limitations toward clinical translation, and prospects (Fig. 2). Initially, we summarize the MN-mediated diverse treatments of skin infections, particularly the integration of MNs with innovative antimicrobial agents (*e.g.*, photosensitizers, sonosensitizers, metals, nanoenzymes, gas molecules, and living bacteria) to provide groundbreaking therapies for severe infections. Furthermore, we focus on the nanoenzyme-based multimodal therapy for chronic infectious wounds, since the nanoenzyme integrates anti-bacterial, anti-inflammatory, and immunomodulatory activities as an "all-in-one" therapeutic strategy to thoroughly address the dynamic and interactive pathogenic factors [27]. In addition, we present the potential of wearable biosensing MNs as a point-of-care medical device in detecting specific pathogens, monitoring disease progression, and tracking drug pharmacokinetics, which will facilitate personalized treatment of skin infections [28]. Moreover, we discuss the current challenges and prospects of antimicrobial MNs to guide the rational design, practical application, and clinical translation of MNs. In general, we hope this review will provide valuable guidance for the future development of antimicrobial MNs.

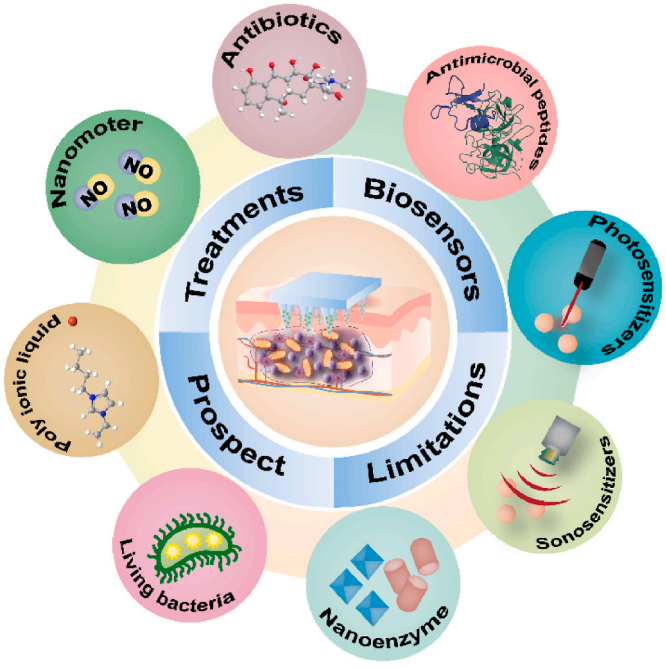

Fig. 2. An overview of MNs used for skin infections, including treatments, biosensors, limitations, and prospect.

2. MNs used to treat bacterial skin infections

Bacteria are the most frequent cause of skin infections [29]. In the past decade, the salient advantages of MNs have spurred massive researches in the MN-mediated topical treatment of bacteria-induced skin infections, such as impetigo, infectious wounds, and acne vulgaris. To date, MNs have been used to load a wide range of therapeutic agents, providing diverse therapies for acute to chronic bacterial infections, such as drug therapy (*e.g.*, antibiotics, antimicrobial peptide), photodynamic therapy (PDT), photothermal therapy (PTT), metal-based antibacterial therapy (MABT), chemodynamic therapy (CDT), sonodynamic therapy (SDT), starvation therapy (ST), nanoenzyme antibacterial therapy (NABT), poly (ionic liquid) (PIL), and combination therapy (Fig. 3).

2.1. Drug therapy

2.1.1. Antibiotics for antibacterial treatment

Antibiotics are the medications used to fight bacterial infections [30]. Initially, the term "antibiotics" refers to the secondary metabolites produced by bacteria, molds, or other microorganisms, such as penicillin produced by the fungus *Penicillium* [31]. Nowadays, this term includes both natural and semi-synthetic chemical substances that have bactericidal (destroy bacterial cells) or bacteriostatic (inhibit bacterial growth) activities [32]. The antibacterial activity of antibiotics was first discovered by Pasteur and Joubert in 1877. Antibiotics have gone through several generations of development to overcome resistance in bacteria. Generally, antibiotics are classified by their mechanisms of action as follows (Fig. 4a): (1) Bacterial cells are surrounded by cell walls made of peptidoglycan. Antibiotics (*e.g.*, vancomycin, telavancin) that act on the different stages of peptidoglycan synthesis and cell wall assembly can cause bacteria to expand, rupture, and die in a low osmotic pressure environment [33]. Therefore, such antibiotics mainly have bactericidal effects on bacteria in the breeding stage rather than the resting stage. (2) Some antibiotics can kill bacteria by disrupting the integrity of cell membranes and increasing the permeability of cell membranes, such as carvacrol [34]. (3) Some antibiotics can induce bacterial death by inhibiting ribosomal protein synthesis, such as chloramphenicol, clindamycin, erythromycin, and azithromycin [35]. (4) Some antibiotics, such as gentamicin sulfate, can inhibit nucleic acid synthesis by binding to bacterial topoisomerase II or inhibiting RNA polymerase. (5) Unlike humans, who get the vitamin from food, bacteria synthesize folic acid by themselves. Therefore, antibiotics that inhibit enzymes involved in folic acid synthesis can cause lethal death to bacteria cells rather than human cells, such as sulfonamides, isoniazid, and so on [36]. Overall, antibiotics are the first-line therapy for bacterial infections in clinical practice.

Compared with injectable or transdermal administration of antibiotics, MN-mediated topical delivery of antibiotics to the site of infection has demonstrated improved antibacterial effects and reduced side effects. In 2010, Gittard et al. [38] prepared gentamicin sulfate-doped antibacterial MNs via a photopolymerization-micromolding technique for the first time and confirmed their antibacterial activity against *Staphylococcus aureus* via an agar plate assay. Since then, MNs have been used to deliver several other antibiotics, including vancomycin [39], carvacrol [40], chloramphenicol [37], and so on, to exert satisfactory antibacterial or antibiofilm activity *in vitro* and *in vivo* (Table 1). With the assistance of MNs, a more significant amount of antibiotics can be delivered to the site of infection for enhanced antibacterial effects, which contributes to reducing antibiotic dose, treatment duration, and potential bacterial resistance. For instance, Ziesmer et al. found that vancomycin delivered by MNs produced a more than 500-fold higher local drug concentration than that administered by intravenous

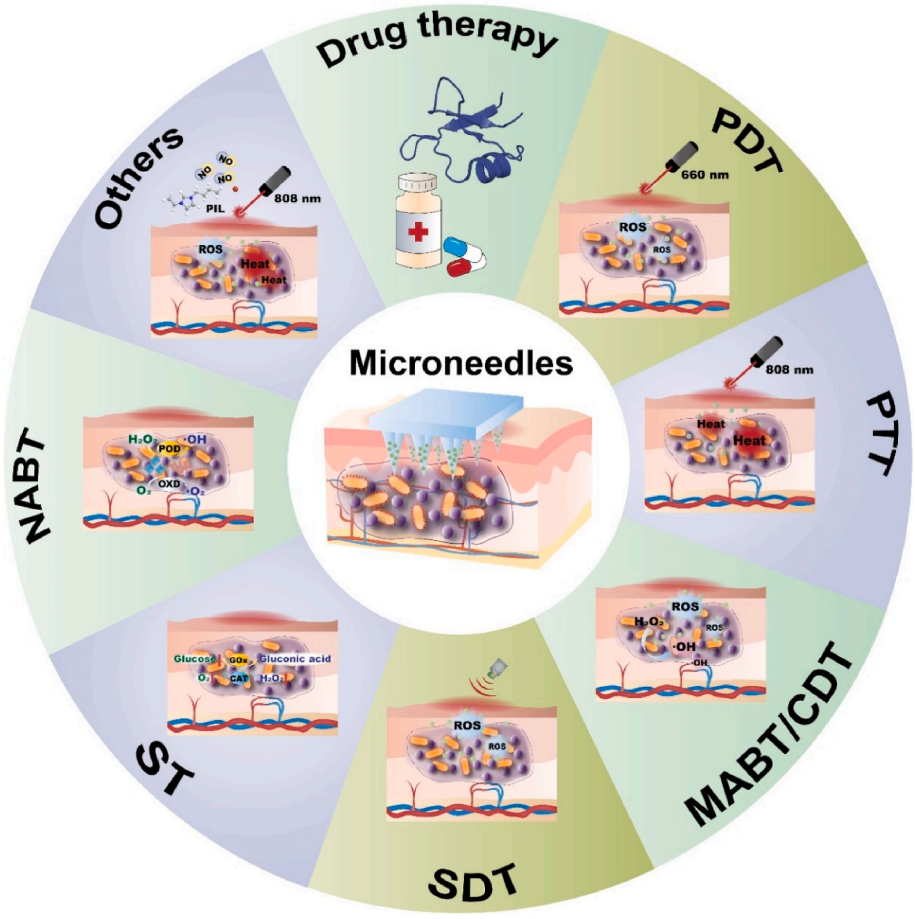

Fig. 3. MN-mediated diverse treatments of bacterial skin infections. PDT: photodynamic therapy; PTT: photothermal therapy; MABT: metal-based antibacterial therapy; CDT: chemodynamic therapy; SDT: sonodynamic therapy; ST: starvation therapy; NABT: nanoenzyme antibacterial therapy; PIL: poly ionic liquid; NO: Nitric oxide; ROS: reactive oxygen species; H_2O_2: hydrogen peroxide; $\bullet O_2^-$: superoxide anion; •OH: hydroxyl radicals; O_2: oxygen; POD: peroxidase; OXD: oxidase; GOx: glucose oxidase; CAT: catalase.

injection [41]. In addition, MNs can enhance the antibiofilm effect of antibiotics by causing physical damage to the biofilm and promoting drug penetration into the biofilms (Fig. 4b–f) [40,37,42]. Unlike healthy surrounding tissues, infected tissues usually have a unique pathological microenvironment, including excessive reactive oxygen species (ROS), low pH, overexpressed specific enzymes, *etc*. Therefore, MNs integrated with drug-loaded responsive nanoparticles (NPs) would enable targeted degradation of NPs and on-demand drug release at the site of infection, thus improving the antibacterial activity of antibiotics [43].

2.1.2. *Antimicrobial peptides for antibacterial treatment*

Antimicrobial peptides consisting of 10 ~ 50 amino acid sequences have emerged as a new class of antimicrobials [47]. As a potential alternative or supplement to conventional antibiotics, antimicrobial peptides have distinct antibacterial mechanisms as follows (Fig. 5a). (1) In general, both natural and synthetic antimicrobial peptides are positively charged and possess an amphiphilic structure, which makes them capable of binding to the negatively charged bacterial membranes via electrostatic interactions. The electrostatic interaction between antimicrobial peptides and cell membranes can cause bacterial lysis, which is widely recognized as a general antibacterial or bactericidal mechanism [48,49]. (2) In some cases, the antimicrobial peptides can also cross the lipid bilayer to inhibit intracellular function, such as inactivating the bioactive substrates such as nucleic acid, proteins, and enzymes [48,49]. (3) Apart from inducing direct bacterial lysis, some antimicrobial peptides can even regulate the host immune response to exert auxiliary antibacterial function, such as recruiting or activating immunocytes to engulf bacteria, increasing the recognition of Toll-like receptors (TLRs) to microbial metabolites, and decreasing inflammatory responses [48]. Multiple factors can influence the antimicrobial activity of antimicrobial peptides, such as charge number, molecular weight, hydrophobicity, compositions and sequences of amino acid, and secondary structures (*e.g.*, α-helix, β-sheet, both α-helix and β-sheet, random coil) [49]. Due to their multi-target antimicrobial activity, antimicrobial peptides offer distinct advantages over traditional antibiotics, including rapid action, reduced drug resistance, broad antibacterial spectrum, and enhanced host immune response [50].

As antimicrobial peptides have a molecular weight of approximately 2000~7000, it is difficult for them to penetrate stratum corneum via conventional transdermal preparations. With the assistance of MN technology, antimicrobial peptides can be delivered to infectious skin tissues. Recently, Su et al. [51] reported antimicrobial peptides (W379)-loaded MNs integrated with a Janus-type antibacterial dressing to eradicate chronic wound biofilms (Fig. 5b). The membrane permeation and depolarization tests demonstrated that the W379 peptide effectively killed both the gram-positive and gram-negative bacteria by targeting their membranes. In addition, the dressing consisting of electrospun nanofibrous membranes helped to eradicate both MRSA biofilms in the type II diabetic mice wound (Fig. 5c) and *Pseudomonas aeruginosa*/MRSA blend films in *ex vivo* human skin wound (Fig. 5d). Therefore, antimicrobial peptides-functionalized MNs hold great potential for treating chronic infectious wounds.

Polymyxin is a kind of natural antimicrobial peptide that is secreted by *Paenibacillus polymyxa*, a dominant bacterial species, to inhibit the

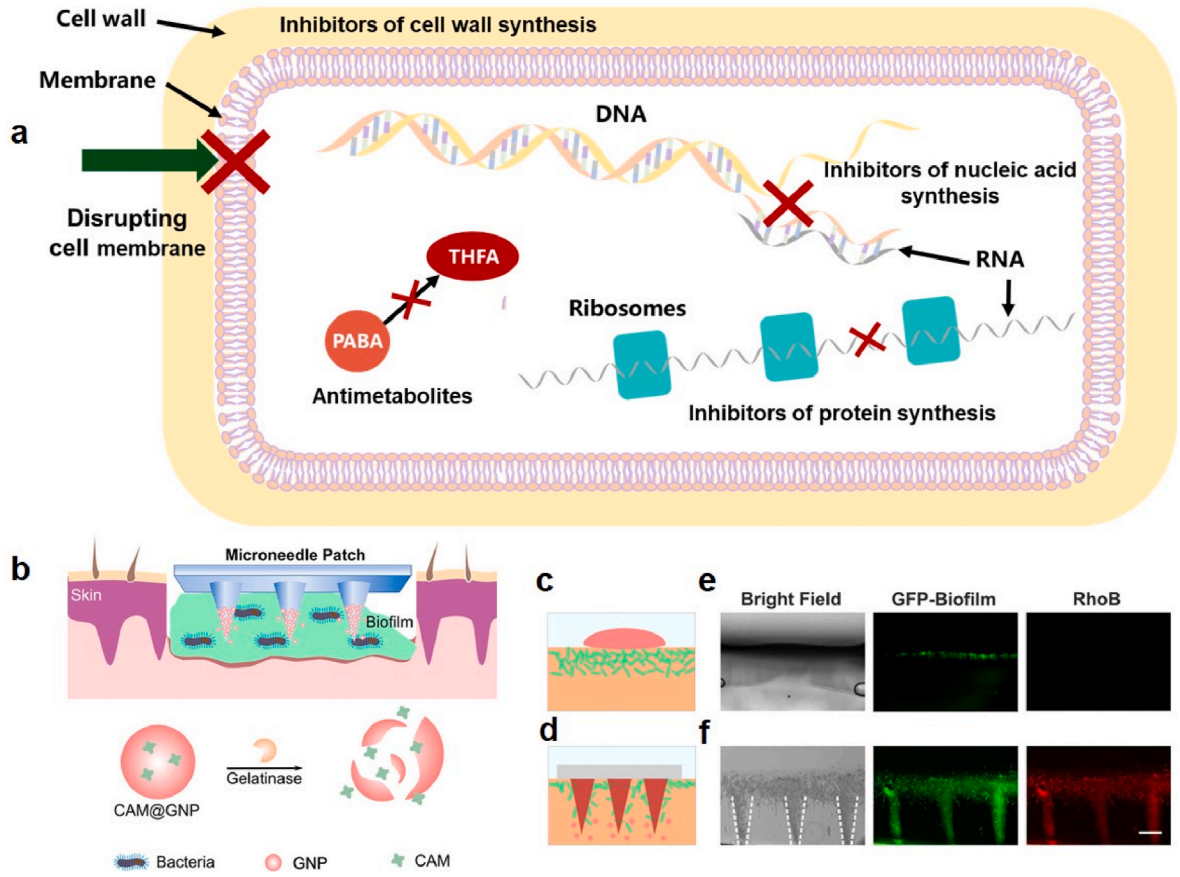

Fig. 4. Antibiotics used for treating skin infections. **(a)** The antibacterial mechanism of antibiotics. PABA: p-aminobenzoic acid; THFA: tetrahydrofolate; DNA: deoxyribonucleic acid; RNA: ribonucleic acid. **(b)** Schematic illustrating the MN-mediated intradermal delivery of chloramphenicol-loaded gelatin NPs (CAM@GNP) to treat biofilm-induced skin infections. The CAM@GNP can be degraded explicitly by active bacteria-secreted gelatinase, thus providing responsive release of CAM at the site of infection and reducing off-target side effects. GNP: gelatin nanoparticles; CAM: chloramphenicol. **(c)** Schematic illustrating the utilization of dye (sulforhodamine B) solution to treat fluorescent protein (GFP)-labeled biofilms. **(d)** Schematics of inserting the sulforhodamine B-loaded MN patch into the skin and the release of dye into biofilms. Fluorescence microscope images displaying the spatial distribution of dye in GFP-labeled biofilms treated with **(e)** solution or **(f)** MN patch. The scale bar is 200 μm. Fig. 4b–f were reproduced from Ref. [37] with permission.

proliferation of other bacteria [52]. Polymyxin has been reported to exert a broad-spectrum antibacterial activity and eliminate the emergence of bacteria resistance [53,54]. Recently, Zhang et al. [55] reported polymyxin-loaded bioinspired MNs for preventing bacterial infection during administration. Each MN patch was equipped with a suction-cup-like structure to mimic the tentacles of an octopus, so that their adhesion ability could be well maintained in any of the dry, moist, and wet environments. Inspired by the adhesive nature of mussel byssi, polydopamine (PDA) was used to prepare a highly adhesive MN base, enabling the MNs to tightly fit the skin and realize self-healing performance. Polymyxin was also loaded in both the tips and base of the MNs to combat common bacteria such as *E. coli*. Taken together, bioinspired MNs with high adhesion ability and antibacterial activity hold great potential for versatile transdermal drug delivery, particularly for mobile joints.

2.2. Photodynamic therapy (PDT)

PDT is an effective antimicrobial therapy that utilizes laser-irradiated photosensitizer to produce cytotoxic reactive oxygen species (ROS) for killing bacteria [56]. Upon laser irradiation, the photosensitizer can be activated to produce highly cytotoxic ROS that cause irreversible damage to the microbial cell membrane, enzymes, proteins, and nucleic acids [57]. The antimicrobial mechanism of PDT is relatively explicit and is generally performed in the following steps (Fig. 6a). (1) First, the photosensitizer absorbs photons, which causes it to transit from a ground state (S_0) to an excited singlet state (S_n) [58]. (2) The intersystem crossing (ISC), then transforms from the unstable S_n into a relatively stable triplet excited state (T_1) [57]. (3) In the T_1 state, photosensitizer can generate ROS by two photochemical reactions. In Type I reaction, the transfer of an electron or hydrogen atom to the surrounding oxygen molecule is usually accompanied by the production of highly cytotoxic oxygenated radicals, including superoxide anion ($\bullet O^{2-}$), hydrogen peroxide (H_2O_2), and free hydroxyl radicals ($\bullet OH$) [59]. In the Type II reaction, the direct reaction between the photosensitizer in the *T1* state and the triplet ground state oxygen ($^3O_2$) leads to the production of highly reactive singlet oxygen ($^1O_2$) [59]. Both reactions can concurrently occur in a photodynamic event and the $^1O_2$ derived from Type II reaction is usually regarded as the key factor for most photosensitizers to exert antibacterial activity due to its relatively more straightforward reaction principle than that of Type I. However, the antimicrobial efficiency of Type II reaction-based PDT relies heavily on the concentration of oxygen, which may hinder its practical application. In contrast to antibiotics, PDT has rapid antibacterial activity and shows potential in treating refractory bacterial infections caused by multidrug-resistant bacteria and biofilms. PDT has gained increasing attention in the antibacterial field owing to its advantages of minimal invasiveness, high efficiency, and few adverse reactions [60]. The practical implementation of both single PDT and PDT-based multimodal antibacterial therapy is detailed below.

Table 1
MNs loaded with various antibiotics to treat bacteria or biofilm-induced skin infections.

Antibiotics	Microneedle design and drug loading	Microneedle geometrics	Evaluation methods	Key findings	Refs
Gentamicin sulfate	Photopolymerized MNs	Conical MNs: 5 × 5 needle arrays; Needle length: 500 μm; Base diameter: 150 μm; Tip angle: 45°.	Agar plating assay	The MNs exerted good antibacterial effect against *S. aureus*.	[38]
Vancomycin	MNs made of drug-loaded water-soluble tips and water-insoluble baseplate; Drug loading: 100 μg per patch	Pyramidal MNs: 10 × 10 needle arrays; Needle length: 600 μm; Base diameter: 200 μm	Agar diffusion tests and *ex vivo* skin infection model	The MNs produced a 500-fold higher local drug concentration than intravenous injection.	[41]
	Hydrogel forming MNs	Conical MNs: 5 × 5 needle arrays; Needle length: 600 μm; Base diameter: 300 μm; Interneedle spacing: 300 μm	Agar plating assay	The MNs displayed excellent antimicrobial performance against *S. aureus*.	[44]
Carvacrol (CAR)	Hollow MNs (AdminPen®) used for delivering responsive CAR-loaded NPs	Circular MNs; AdminPen® 777: 121 needle numbers and 700 μm needle length; AdminPen® 1200: 43 needle numbers and 1100 μm needle length; AdminPen® 1500: 31 needle numbers and 1400 μm needle length	*Ex vivo* biofilm model	AdminPen® 1500 was the most effective device in enhance drug delivery efficiency and prolong drug retention at the site of infection.	[40]
Chloramphenicol (CAM)	Dissolving MNs loaded with gelatinase-sensitive gelatin NPs	Pyramidal MNs: 15 × 15 needle arrays; Needle length: 600 μm; Base diameter: 200 μm; Interneedle spacing: 500 μm	*In vitro* biofilm-infected wound model	The MNs directly penetrated the biofilm matrix and dissolved to release CAM-loaded NPs, which further disassembled to release CAM for eradicating biofilm.	[37]
	Dissolving MNs loaded with bacteria-sensitive microparticles; Drug loading: 70.58 μg per patch	Pyramidal MNs; Needle length: 700 μm; Base diameter: 200 μm	*In vitro* and *in vivo* mutant Drosophila larval infection model	The composite MNs, could killed 99.99 % of bacterial bioburdens.	[45]
Clindamycin	ROS-responsive MNs supported by a substrate with high physical adsorption capability	Conical MNs: 11 × 11 needle arrays; Interneedle spacing: 600 μm	Agar plating assay and *P. acnes*-infected mouse model	The needles provided ROS-responsive and continuous release of drug in the acne area, while the substrate absorbed pus and dead cell debris to accelerate the healing of skin.	[43]
	Stimulus responsive dissolving MNs	Pyramidal MNs; Needle length: 870 μm	Measurement of bacterial inhibitory zones and biofilm-infected wounds	Clindamycin microfibers-coated MNs provided on-demand drug release and effective treatment of cutaneous bacterial biofilms.	[46]
Erythromycin or azithromycin	Dissolving MNs	Pyramidal MNs: 10 × 10 needle arrays; Needle length: 870 μm	Agar plating assay and biofilm-infected wounds	Azithromycin-loaded MNs were effective in treating wound biofilms.	[42]

2.2.1. Single PDT

Caffarel-Salvador et al. [62] developed methylene blue-loaded dissolving MNs with enough mechanical strength to treat infectious wounds. When the concentration of methylene blue was adjusted to follow the range of delivered dose by the MNs (0.1–2.5 mg/mL), the biofilm incubated with methylene blue was subjected to irradiation at 635 nm using a Paterson lamp for determining the bacterial killing rate. The total bacterial viability count demonstrated that the methylene blue-mediated PDT killed >96 % of *S. aureus* and >99 % of *E. coli* and *C. albicans*, showing excellent antibacterial effects. As most of the photosensitizers are water-insoluble and have poor penetration in dense biofilms, the antibiofilm effects of PDT are usually very limited. To address the poor solubility and penetration in the biofilms of photosensitizers, Wang et al. [63] synthesized sulfobutylether-β-cyclodextrin (SCD)/tetra(4-pyridyl)-porphine (TPyP) supramolecular photosensitizers and loaded them in MNs for improving the antibiofilm effect of PDT. The inclusion complex of TPyP and SCD effectively reduced the aggregation of the photosensitizers and enhanced the penetration of the photosensitizers to the biofilms, resulting in a nearly tenfold increase in the productivity of ROS. The TPyP/SCD-based MNs had sufficient mechanical strength to pierce the EPS of the biofilm, enabling topical delivery of the photosensitizers to the biofilm and further PDT-mediated ablation of the biofilm. Furthermore, the *in vivo* antibiofilm activity of the TPyP/SCD-based MNs was confirmed in *S. aureus*-infected mice with obvious abscesses.

Compared to organic photosensitizers, inorganic photosensitizers possess higher photostability and unique photocatalytic activity, which makes them available for repeatable PDT and photocatalytic-amplified antibacterial PDT. In addition, some inorganic photosensitizers may even eliminate the requirement of sufficient oxygen supply to achieve repeatable PDT and produce continuous ROS. To this end, Gong et al. [64] developed $Zn_2GeO_4:Cu^{2+}$ (ZGC) luminescence nanorods with long-persistent photocatalytic effect for continuous ROS production. The ZGC nanorods were loaded in the MNs (ZGC@MNs) for direct delivery to the biofilms and treatment of MRSA-infected wounds. After pre-illumination, the ZGC released from the MNs exhibited long-lasting photocatalysis for consistent ROS production over 48 h, resulting in excellent antibacterial activity. Accordingly, pre-illuminated ZGC@MNs efficiently eliminated MRSA biofilm to reduce the inflammation level and accelerate the healing of MRSA-infected wounds established in BALB/c mice.

2.2.2. PDT-based multimodal therapy

As the therapeutic efficiency of a single PDT is often limited by the penetration depth of the laser and insufficient oxygen supply, the combination of PDT and other antibacterial agents (*e.g.*, metal ions, antimicrobial peptide) has emerged as a preferred approach to improve antibacterial effect by initiating complementary antibacterial activities. Acne vulgaris is a prevalent chronic inflammatory skin disease affecting over 80 % of the global population, particularly adolescents. Wen et al. [61] developed MNs integrated with zeolitic imidazolate framework-8 (ZIF-8) NPs for chemo-photodynamic treatment of acne vulgaris (Fig. 6b). In this study, ZIF-8 NPs were first prepared to load indocyanine green (ICG) for improving the photostability of ICG, and then mixed with HA gel to manufacture hybrid MNs. The MNs directly penetrated the EPS of the biofilm to deliver the ICG-loaded ZIF-8 NPs inside. The infected tissues were then irradiated with an 808 nm laser to produce massive ROS for inhibiting the excessive proliferation of *P. acnes*. Zn^{2+}

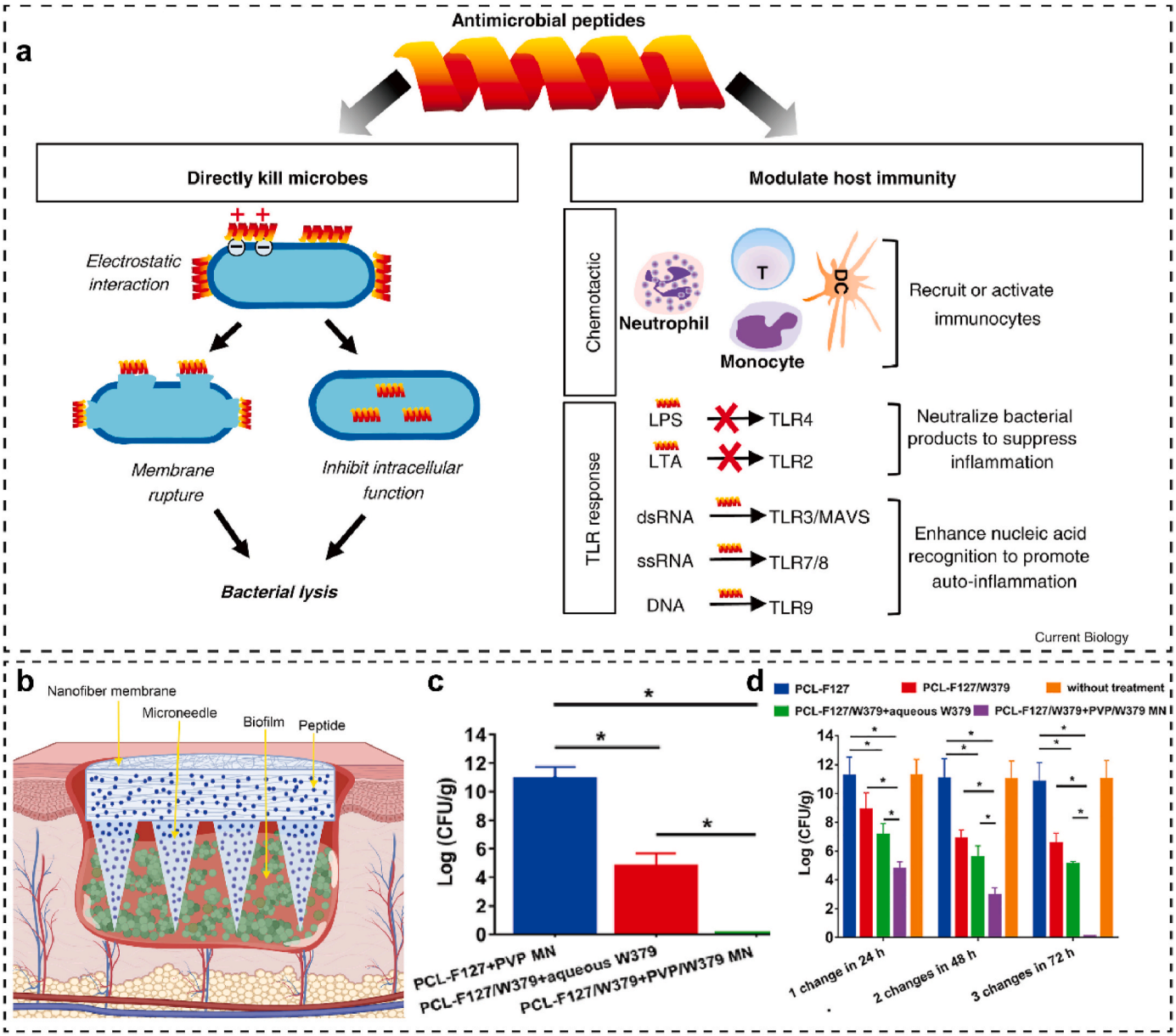

Fig. 5. Antimicrobial peptides used for treating skin infections. **(a)** The antibacterial mechanism of antimicrobial peptides, including direct bacterial killing and modulating host immunity. Adapted from Ref. [48] with permission. **(b)** Development of W379 peptide-loaded MNs integrated with Janus-type antimicrobial dressings to treat biofilm-infected chronic wounds. *In vivo* anti-biofilm efficacy of W379 and Janus-type antimicrobial dressings against the biofilm-infected wounds established on the **(c)** type II diabetic mice and **(d)** *ex vivo* human skin. Adapted from Ref. [51] with permission.

was further sustainably released from the ZIF-8 reservoir to destroy the bacterial membrane through electrostatic interaction force and electron transfer-induced ROS generation. The bactericidal rate of combined treatment with PDT and Zn^{2+} against *P. acnes* was 99.76 %, which contributed to reduced skin thickening, redness, and inflammation in the acne mouse model (Fig. 6c-d). Lei et al. [65] reported the chemical conjugation of chlorin e6 (Ce6) with antimicrobial peptide (AmP-Ce6, AC) to exert synergistic antibacterial effects. AC was formulated into zwitterionic micelle (DPP@AC) by self-assembling with a pH-responsive tri-block polymer (DMA–PEI–PLGA) to improve the solubility of Ce6. The DPP@AC micelle was further mixed with hyaluronic acid meth-acryloyl (HAMA) gel to fabricate MN patches for the responsive release of antibacterial agents in the skin. Under acidic conditions, the DAP group was protonated to induce the charge conversion of the micelle from negative to positive charge, which enabled the exposure of positively charged AmP for targeted bacterial killing. DPP@AC demonstrated a higher bactericidal activity against *S. aureus* biofilms at a lower pH *in vitro*, resulting in an MIC_{90} value of <5 μM and a biofilm eradication rate of 90 % under laser irradiation. The synergistic antibacterial effect of AmP and Ce6-mediated PDT was also confirmed in diabetic mice bearing *S. aureus* biofilm-infected wounds, which completely healed within 15 days.

2.3. Photothermal therapy (PTT)

PTT utilizes laser-irradiated photothermal agents to convert light energy into heat for bacterial killing [66]. The explicit antibacterial mechanism of PTT includes two aspects (Fig. 7a): (1) Generate hyperthermia to disrupt bacterial integrity, such as damaging the structure of cell membrane and bioactive substances (*e.g.*, DNA, proteins, enzymes) [67]; (2) Activate host immune response, such as recruiting immune cells (*e.g.*, macrophages and neutrophils) to combat bacterial infections

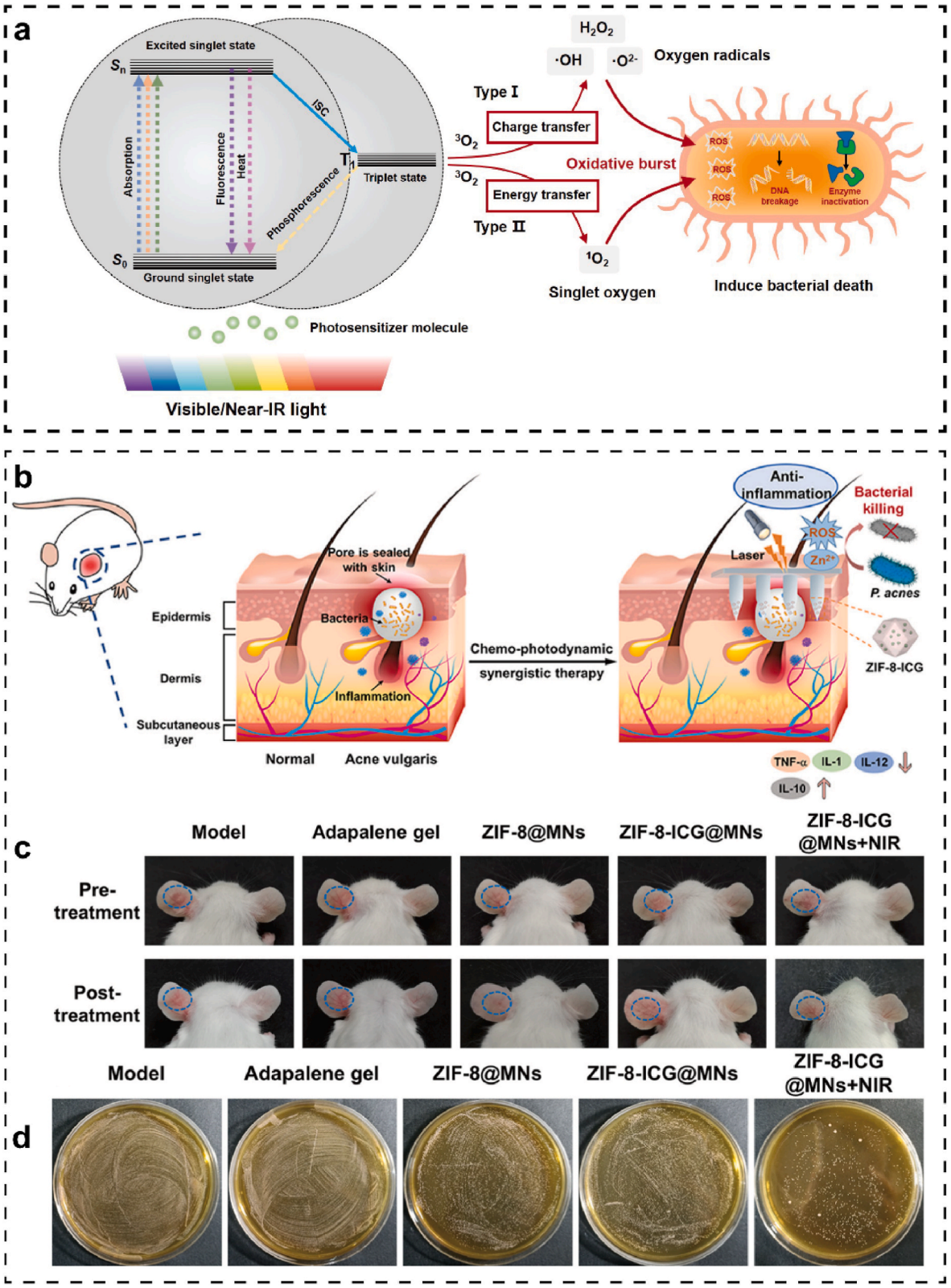

Fig. 6. PDT used for skin infections. **(a)** Antibacterial mechanism of PDT. S_0 and S_n refer to the ground and excited singlet state of the photosensitizer molecule, respectively; ISC: intersystem crossing; T1: triplet excited state of the photosensitizer molecule; $^3O_2$: ground state oxygen; $^1O_2$: singlet oxygen; $\bullet O^{2-}$: superoxide anion; •HO: hydroxyl radical; H_2O_2: hydrogen peroxide. **(b)** Schematic illustration of MNs bearing ICG-loaded ZIF-8 for chemo-photodynamic therapy against acne vulgaris. **(c)** Representative images to show the appearance alterations in the *P. acnes*-infected ear before and after treatment. **(d)** Photographic images of the bacterial colonies harvested from the infectious ear showed the antibacterial effect of different treatments. Adapted from Ref. [61] with permission.

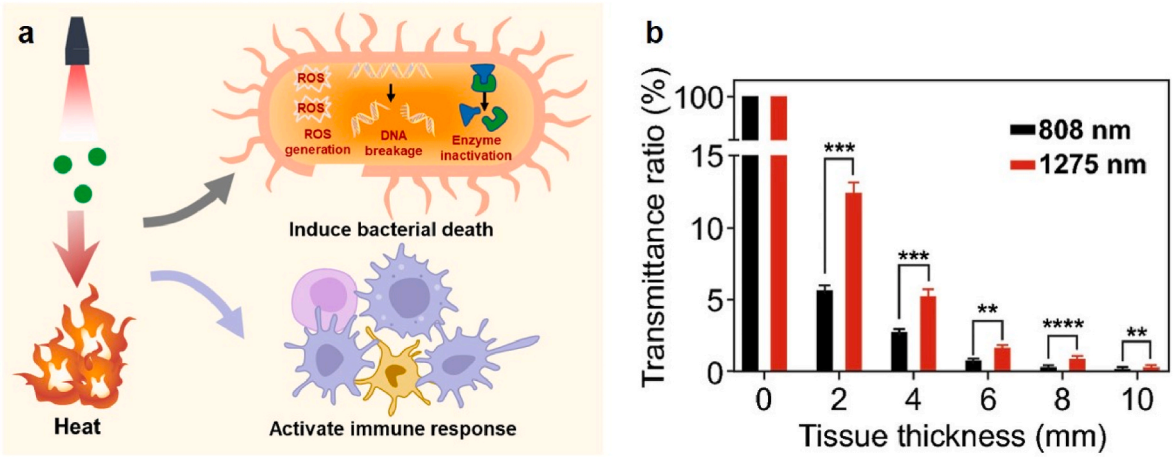

Fig. 7. PTT used for skin infections: **(a)** Antibacterial mechanism of PTT. **(b)** The transmittance ratio of 808 and 1275 nm laser penetrating the porcine muscle with different thicknesses. Adapted from Ref. [70] with permission.

[68]. Compared to antibiotics, PTT can target multiple cellular components and reshape the immune environment, endowing it with distinct advantages such as broad-spectrum antimicrobial activity against various pathogens, short treatment time (just a few minutes), and negligible bacterial resistance [69]. PTT can also elevate local temperature to enhance the permeability of the biofilms, thus effectively eradicating biofilms. The wavelength of light irradiation located in the near infrared Region II (NIR-II, 1000–1700 nm) biological window usually has higher tissue penetration depth (up to 2–3 cm) than that of near infrared Region I (NIR-I, 650–900 nm) (0.5–1 cm) (Fig. 7b) [70,71]. Therefore, the antibacterial performance of PTT can be enhanced by changing the wavelength of the light source, and NIR-II-based PTT might be a more effective alternative to treat severe skin infections. MN-mediated photothermal antibacterial therapy has captured much attention in the field of skin infection because of the combined benefits of PTT and MNs. Detailed examples are shown below.

2.3.1. *Single PTT*

More than 90 % of chronic wounds are reported to be infected with biofilms, which can induce excessive and prolonged release of proinflammatory cytokines to prevent wound healing. *S. aureus* is one of the common bacteria present in chronic wounds and can specifically secrete gelatinase. To treat chronic wounds infected with *S. aureus* biofilm, Lei et al. [72] developed an antibacterial MN patch that is loaded with gelatinase-responsive release of photothermal peptide (AMP-Cypate). Gelatin NPs (GNPs) were synthesized and conjugated with AmP–Cypate to prepare AMP-Cypate@GNPs, which can be specifically degraded by gelatinase to afford responsive release of AMP-Cypate in the infectious wounds. AMP-Cypate@GNPs was further loaded in the needle tips of MNs prepared from poly (vinylpyrrolidone) (PVP K30) and recombinant Type III collagen protein. When applied to the infection site, the MNs pierced the skin tissues and delivered Cypate@GNPs to the biofilms. Then, Cypate@GNPs were degraded by overexpressed gelatinase present in the infection site to provide responsive release of AMP-Cypate for photothermal antibacterial therapy. The ability of Cypate@GNPs laden MNs to treat chronic wounds was confirmed in the staphylococcal infection-induced mice with diabetic foot ulcers. However, single PTT usually necessitates high temperature (>60 °C) and long irradiation time to kill bacteria and prevent bacteria rehabilitation, which causes inevitable thermal damage to surrounding healthy tissues during treatment [73]. To prevent high temperatures from damaging normal tissues, mild PTT with a temperature less than 50 °C has been regarded as an alternative antibacterial therapy [74]. However, the antibacterial effect of a single mild PTT is severely limited by the specificity and penetration depth of laser irradiation [67]. Therefore, accumulating research has proposed the combination of mild PTT with other antimicrobial agents (*e.g.*, antimicrobial peptides, antibiotics, nanomoters) to achieve synergistic antibacterial effects with minimized adverse reactions (Fig. 8).

2.3.2. *PTT-based multimodal therapy*

Benefiting from the unique antibacterial activity of antimicrobial peptides, the integration of photothermal MNs with antimicrobial peptides has demonstrated great potential in affording synergistic antibacterial effects. In a recent study reported by Su et al. [77], a photothermal MN patch loaded with antimicrobial peptides (W379 peptide) was developed to manage biofilm-infected wounds. IR 780 and W379 peptides were first co-loaded in PVP MNs, which were then coated with 1-tetradecanol (TD) as a phase transition material. Upon exposure to NIR irradiation at 808 nm, IR780 produced hyperthermia to melt TD, further accelerating the dissolution of the MNs and release of the W379 peptide in the infected wounds. Compared with conventional MNs, the NIR-responsive MNs demonstrated superior *in vitro* and *in vivo* antibiofilm activities, showing great potential for treating biofilm-infected wounds. In another research reported by Feng et al. [75], an antimicrobial peptidomimetics (4 K10)-augmented photothermal and photocatalytic MN patch was devised for the treatment of skin infections (Fig. 8a). This study constructed a vanadium carbide (V2C) MXene-based two-dimensional nanosheet as a novel photothermal agent with a dual function of photothermal and photocatalytic activities. Particularly, the degradation product of V_2C exerted persistent photocatalytic performance to inhibit potential bacterial rebound. Further, 4K10 with a membranolytic nature was electrostatically coated onto the V_2C Mxene (4 K10@V_2C) to achieve multiple antibacterial activities for enhanced therapeutic outcomes. The *in vitro* antimicrobial activity test demonstrated that >99.9 % of MRSA and *P. Aeruginosa* were killed by the 4 K10@V_2C nanosheets at a photothermal temperature of 54.1 °C. The 4 K10@V_2C nanosheets also eliminated >99.98 % of MRSA biofilms in the *ex vivo* human skin infection model. Taken together, the 4 K10@V_2C nanosheets-loaded MNs with integrated membranolytic, photothermal, and photocatalytic activities hold substantial potential for treating skin infections.

The combination of PTT and antibiotics is another effective approach to improve antibacterial effects. Although MNs are effective in piercing the interior of biofilms, the compact and viscous EPS involved in biofilms severely impedes the diffusion and permeation of actives to reach the bacterial cell, making the bacteria insusceptible to therapy. In view of this, Yu et al. [76] developed dissolving MNs integrated with α-amylase and levofloxacin-loaded PDA NPs (PDA@Levo) to provide enzymolytic, antibiotic, and photothermal triple therapies against wound biofilms (Fig. 8b). The *in vitro* antibiofilm test showed that the

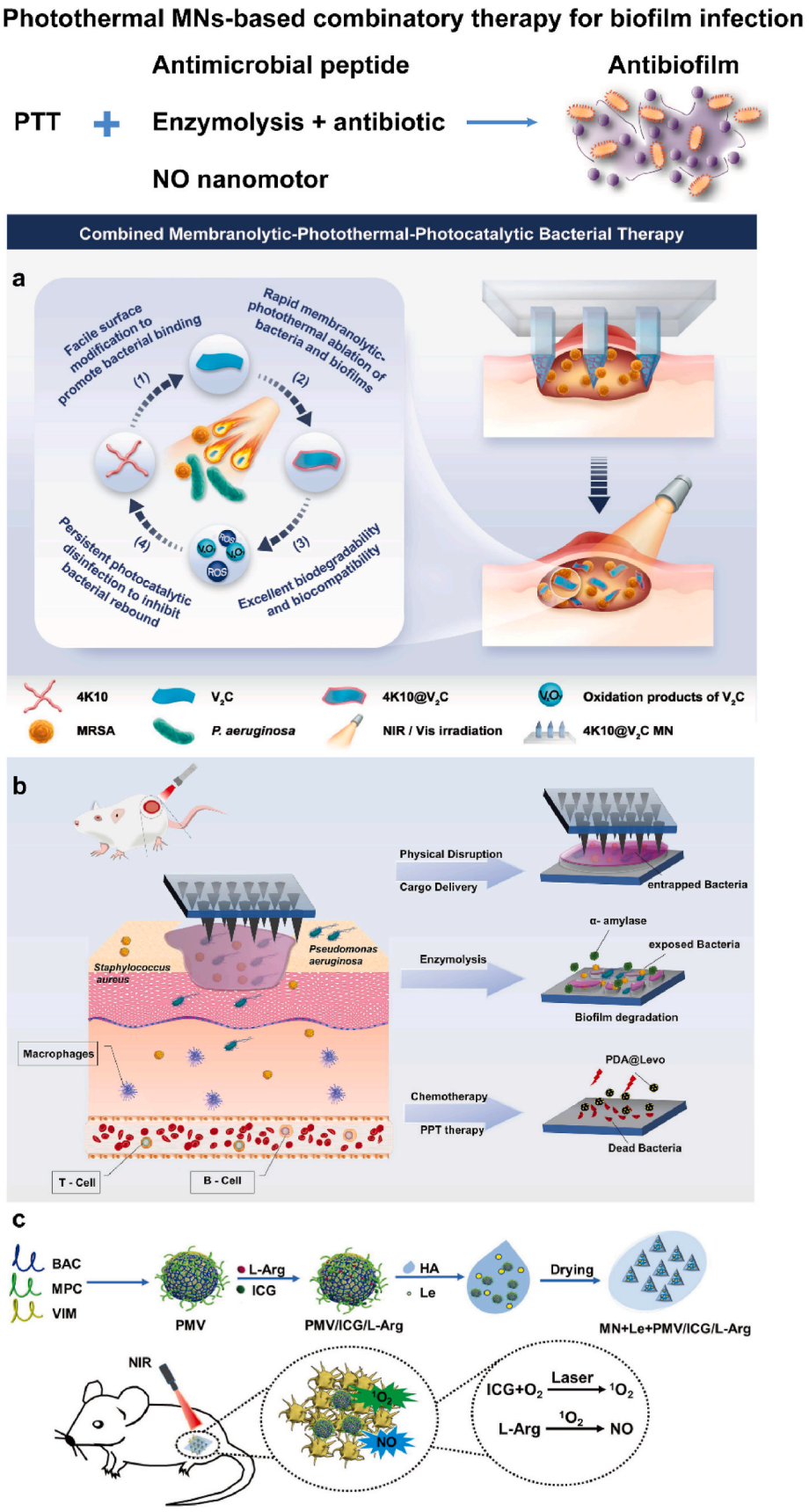

Fig. 8. Photothermal MNs-based combinatory therapy for biofilm infection: **(a)** Construction of 4 K10@V_2C-loaded MNs for membranolytic, photothermal, and photocatalytic triple therapy of skin bacterial infections. Adapted from Ref. [75] with permission; **(b)** Dissolving MNs loaded with α-amylase and PDA@Levo for the triple therapy of enzymolysis, chemotherapy, and PTT in biofilm-infected wounds. Adapted from Ref. [76] with permission; **(c)** The preparation process and antibiofilm mechanism of nanomotors-loaded MN patches used for biofilm-infected wounds. Adapted from Ref. [17] with permission.

triple therapy decreased the biomass of *S. aureus* and *P.aeruginosa* biofilms to 12.6 % and 31.3 %, respectively. After application of the multifunctional MNs for 10 min, the full-thickness and biofilm-infected wounds were exposed to 808-nm NIR irradiation for accelerated dissolution of the MNs and further release of α-amylase. Afterward, α-amylase degraded the EPS to expose the bacteria to levofloxacin and PTT, thus eliminating the biofilms and lowering the inflammation level to accelerate wound healing. After receiving the MN-mediated multimodal therapy for 11 days, the infected wounds were almost completely healed.

Although PTT and α-amylase can damage EPS and enhance the penetration of antimicrobials into the biofilm, the space between MNs and bacteria makes it challenging for antimicrobials to reach all the bacteria. The residual bacteria will continue to proliferate, resulting in treatment failure. The increase in the contact area between bacteria and antimicrobials may enhance the antibiofilm effects. Accordingly, Chen et al. [17] developed nanomoter-integrated MN patches to drive the motion of antimicrobials toward bacteria for enhanced treatment of biofilm-infected wounds (Fig. 8c). Specifically, luteolin (Le) was used as a bacterial quorum sensing inhibitor to prohibit the growth of biofilm, while ICG and L-arginine (L-Arg) were co-loaded in the nanomotors to provide the source of movement. Le and nanomoters were then mixed with HA gel to prepare nanomotor-propelled MNs. Under NIR irradiation, ICG could not only generate hyperthermia as an autothermal power force to drive the movement of the nanomotors, but also produce $^1O_2$ to facilitate the conversion of L-Arg into NO as a pneumatic force. The dual autothermal power and pneumatic force enabled nanomotors to permeate into deeper biofilm, contributing to more efficient elimination of the bacteria present in the biofilms by disrupting bacterial membranes and inducing the leakage of cytoplasm. The pharmacodynamic studies on rat wounds inoculated with *S. aureus* biofilms further demonstrated that the nanomotor-propelled MNs showed the best antibiofilm activity and promoted wound healing most efficiently. Taken together, the nanomotor-propelled MNs provide a multimodal antibacterial therapy integrating Le, PTT, PDT, and NO for biofilm-infected wounds, offering a meaningful strategy to address the poor drug delivery efficiency involved in biofilm infections.

2.4. Metal-based antibacterial therapy (MABT)

Metals have been used as antimicrobial agents for a long history, which have not been replaced by organic antibiotics until the mid-20th century [78]. For instance, the application of silver (Ag) in coins and cutlery can date back to about 7000 years [79]. Most of the antimicrobial metals belong to the d-block transition metals, such as Ag, zinc (Zn), copper ions (Cu), ferrous (Fe), gold (Au), and the like. In many cases, metals are used in the form of ion, NPs, and oxide to exert antibacterial activities in the following ways (Fig. 9): (1) Electric field adsorption sterilization: the metal cations (derived from their original salt or release of NPs) or NPs (*e.g.*, Ag NPs) can bind to the negatively charged cell wall and membrane via electrostatic adsorption, causing the damage of membrane, shrinkage of cytoplasm, and leakage of cellular components. They can further infiltrate into bacteria and interact with intracellular bioactive substances, leading to the loss of cellular function [80]. (2) Induce oxidative stress: the metal ions or NPs can catalyze the oxygen to produce free radicals (*e.g.*, $\bullet O^{2-}$, HO•, H_2O_2) and disrupt the ROS scavenging mechanisms by directly attaching to the thiol groups present in specific enzymes and glutathione disulfide (GSSG), causing oxidative stress damage to bacteria [80,81]. (3) Photocatalysis-mediated sterilization: under ultraviolet irradiation, large amounts of free radicals are produced at the surface of metallic oxide nanoparticles, such as ZnO NPs and TiO_2 NPs, thus exerting antimicrobial effect [82].

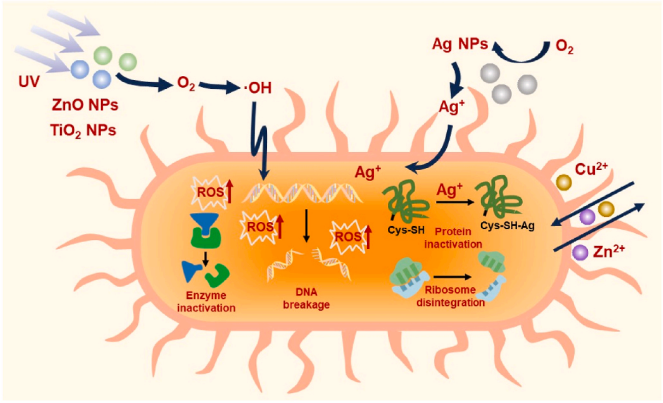

Fig. 9. Antibacterial mechanism of metal in the form of ions, oxide, and NPs.

2.4.1. Single metal-based antibacterial therapy

Both Zn^{2+} and zinc oxide (ZnO) have broad-spectrum activity and are widely used for antibacterial therapy, as they can produce ROS to destroy the proteins and cell walls of bacteria [83]. Gittard et al. [84] prepared acrylate-based solid MNs that were coated with silver or ZnO films. The agar diffusion test demonstrated that the coated MNs had good antibacterial activity against *Staphylococcus epidermidis* and *S. aureus*. Further, Yao et al. [85] developed ZIF-8 laden photocrosslinked methacrylated HA (MeHA) MNs and investigated how the roughness of ZIF-8 affected their antimicrobial activity. ZIF-8 is a classical type of MOFs formed by the self-assembly of Zn^{2+} in coordination with imidazole. In this study, $Zn^{2+}$was released from ZIF-8 to destroy the integrity of the bacterial capsule and convert oxygen molecules into oxygen free radicals, thus efficiently killing *E. coli* and *S. aureus* to promote wound healing. Interestingly, the antibacterial activity of ZIF-8 was enhanced by increasing the roughness of ZIF-8 surface as a result of increased contact area between the MOFs and bacteria. As Ag^+ has excellent antibacterial activity against both gram-negative and gram-positive bacteria [86], González García et al. [87] developed the first generation of AgNPs-loaded dissolving MNs for self-sterilization. The prepared MNs showed good mechanical properties, rapid dissolution behavior, and excellent antibacterial activity. With the release of AgNPs from the MNs, the proliferation of bacteria could be well inhibited at an optimal dosage, which is safe for mammalian cells.

With the delicate design of MNs, metal-based antibacterial therapy has achieved great success in promoting the healing of infected wounds. Inspired by the structure of lamprey teeth, Deng et al. [88] developed an oriented antibacterial sericin MN (OASM) system that contained ZnO NPs to manage infected wounds. The oriented structure of MN arrays provided directional traction force to facilitate wound closure, while the ZnO NPs released from the MNs killed the bacteria by producing ROS and increasing bacterial membrane permeability, thus accelerating infectious wound healing. Although metallic NP-loaded MNs have demonstrated certain antibacterial activities to reduce skin infection, there remains a need to address the problems of low loading capacity, non-uniform distribution, and complex processing parameters of such MNs prepared via conventional microperfusion or coating techniques [89]. Recently, Lu et al. [89] proposed a straightforward Langmuir-Blodgett (LB) technique for preparing antibacterial MNs by depositing metallic NPs (*e.g.*, ZnO NPs, SiO_2-Ag, and ZIF-8) with varying sizes, shapes, and compositions onto the poly (lactic-co-glycolic acid) (PLGA)-based MNs. Compared with the conventional dip coating technique, the LB coating technique offered distinct advantages in controlling the coating layers and providing homogeneous and high coverage without sacrificing the drug loading capacity and release behavior. Consequently, the antibacterial MNs prepared via the LB technique demonstrated superior and prolonged antibacterial performance *in vitro* and *in vivo*, showing great potential for long-term transdermal drug delivery.

2.4.2. CDT-based multimodal therapy

In the presence of H_2O_2, metal ions can catalyze H_2O_2 to produce highly toxic •OH via a Fenton or Fenton-like reaction for bacteria killing, which is also termed as CDT. The concept of CDT was first proposed by Shi and his coworkers in 2016, who developed CDT as a novel anticancer therapy [90]. Fe^{2+} and Fe_2O_3 are the two commonly used CDT reagents. The antibacterial mechanism of CDT is to destroy cell membranes and bioactive substances (*e.g.*, nucleic acids, proteins, and enzymes) by ·OH, which finally causes lethal damage to bacteria. In addition, the ability of ·OH to increase the permeability of bacterial membranes can help CDT sensitize other treatments. Compared to antibiotics, CDT rarely produces bacterial resistance as it can cause irreversible oxidative damage to vital bioactive substances.

Although CDT has shown a broad-spectrum antibacterial activity, its therapeutic efficiency is mainly restricted by the local concentration of H_2O_2 and the inherently insufficient catalytic performance of CDT reagents [91]. The elevation of local temperature can accelerate the Fenton or Fenton-like reaction, thus enabling a synergism of CDT and PTT for enhanced antibacterial effects [92]. In infectious wounds, the polarization of macrophages into the M1 subtype and excessive release of pro-inflammatory factors can cause chronic inflammation, which is an essential contributor to refractory wounds [93]. To enhance the antibacterial performance of CDT and reduce inflammation levels in the wounds, Li et al. [27] developed composite MM patches loaded with antibacterial and immunomodulatory oxide-based NPs to manage infectious wounds (Fig. 10). In this study, PDA and Fe_2O_3 were first used to prepare PDA-loaded NPs (Fe/PDA) with a mean particle size of 110 nm. Glucose oxidase (GOx) was grafted onto the surface of Fe/PDA through an acylation reaction, followed by coating with HA to improve the water dispersibility and stability of the NPs. The resultant Fe/PDA@GOx@HA NPs with an average diameter of 170 nm and amine-modified mesoporous silica NPs (AP-MSN) were further loaded in the tips and backing layer of the MNs, respectively. The Fe/PDA@GOx@HA NPs showed both GOx and peroxidase (POD)-like catalytic properties. Under the weakly acidic and high glutathione (GSH) conditions involved in the infected wounds, the Fe/PDA @GOx@HA NPs were decomposed, releasing GOx, iron ions, and PDA. GOx catalyzed glucose to produce glucuronic acid and H_2O_2, which provided the substrate for iron ions to generate ·OH for bacteria killing. The PDA with an excellent photothermal conversion property enabled PTT upon the laser irradiation at

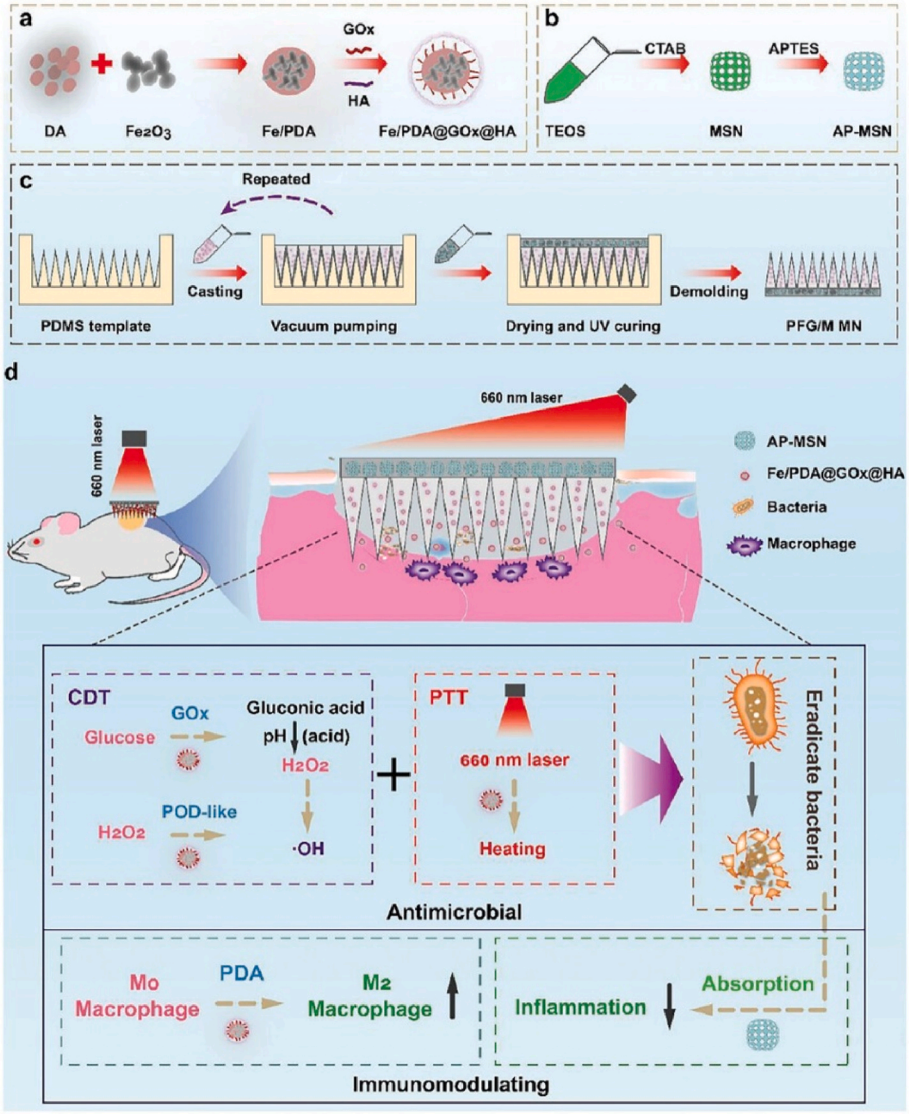

Fig. 10. Development of PFG/M MN for treating infected wound healing: (**a-c**) schematic illustration of preparing **(a)** Fe/PDA@GOx@HA, **(b)** (AP-MSN), and **(c)** PFG/M MN, **(d)** Therapeutic mechanism. TEOS: tetraethyl orthosilicate; CTAB: cetyltrimethylammonium bromide; APTES: 3-aminopropyltriethoxysilane. Adapted from Ref. [27] with permission.

808 nm. The combination of CDT and PTT was effective in eradicating bacteria and promoting the polarization of macrophages into the M2 anti-inflammatory phenotype for enhanced wound repair. Furthermore, the MSNs absorbed pro-inflammatory factors (*e.g.*, free nucleic acids), helping to reshape the inflammatory immune environment and accelerate wound healing. After treatment with the "all-in-one" MM patches for 14 days, the *S. aureus*-infected wounds in mice completely healed.

2.5. SDT and SDT-based multimodal therapy

SDT refers to the utilization of non-thermal ultrasound (US) to activate a sonosensitizer for therapeutic purposes [94,95]. Although extensive researches have been conducted to define the mechanism of SDT, the exhaustive process of how the US activates the sonosensitizers has not been fully understood yet. At present, the cavitation effects caused by the interaction between the US and a liquid medium are regarded as the most convincing explanation. In detail, the cavitation effects are defined as the nucleation, growth, and explosion of bubbles under US irradiation [96,97] (Fig. 11a). During the process of bubble explosion, huge energy can be produced to trigger a pyrolysis-like reaction, which can generate an ultrahigh temperature (>5000 K) and pressure (>103 atm) in the cavitation center [96] (Fig. 11a). In addition, the energy can be transformed into light, which is termed as sonoluminescence, to activate the sonosensitizer for ROS generation via "hole–electron'' pairs or intersystem crossing (ISC) [98] (Fig. 11a). Accordingly, the antibacterial activity of SDT is a collection of sonomechanical, sonothermal, and sonochemical effects, which can disrupt cell walls, increase cell membrane permeability, and inactivate bioactive substances to induce bacterial death.

Compared with PDT, SDT is more effective in eradicating bacterial infections, particularly those seated deep in the skin or muscle, owing to the following reasons: (1), The energy of ultrasound can penetrate the tissues at depths exceeding 10 cm, which is significantly larger than that of NIR light (<3 cm) [99]; (2) The antibacterial activity of PDT-derived ROS is usually compromised by the short half period and effective radius of ROS [94]. However, the antibacterial activity of SDT does not only depend on ROS-induced cytotoxicity, but also on cavitation-mediated sonomechanical and sonothermal effects [100]. SDT has captured much attention as a promising antimicrobial therapy, owing to its noninvasive feature, high tissue penetration, and extensive clinical application basis [101].

TiO_2 is a common inorganic sonosensitizer used for SDT, while it has low ROS productivity owing to the rapid combination of electron (e^-) and hole (h^+) [102]. Recently, several decorated TiO_2 NPs and other alternative sonosensitizers have been explored to achieve more efficient SDT. Ouyang et al. [103] used crystal engineering to explore the

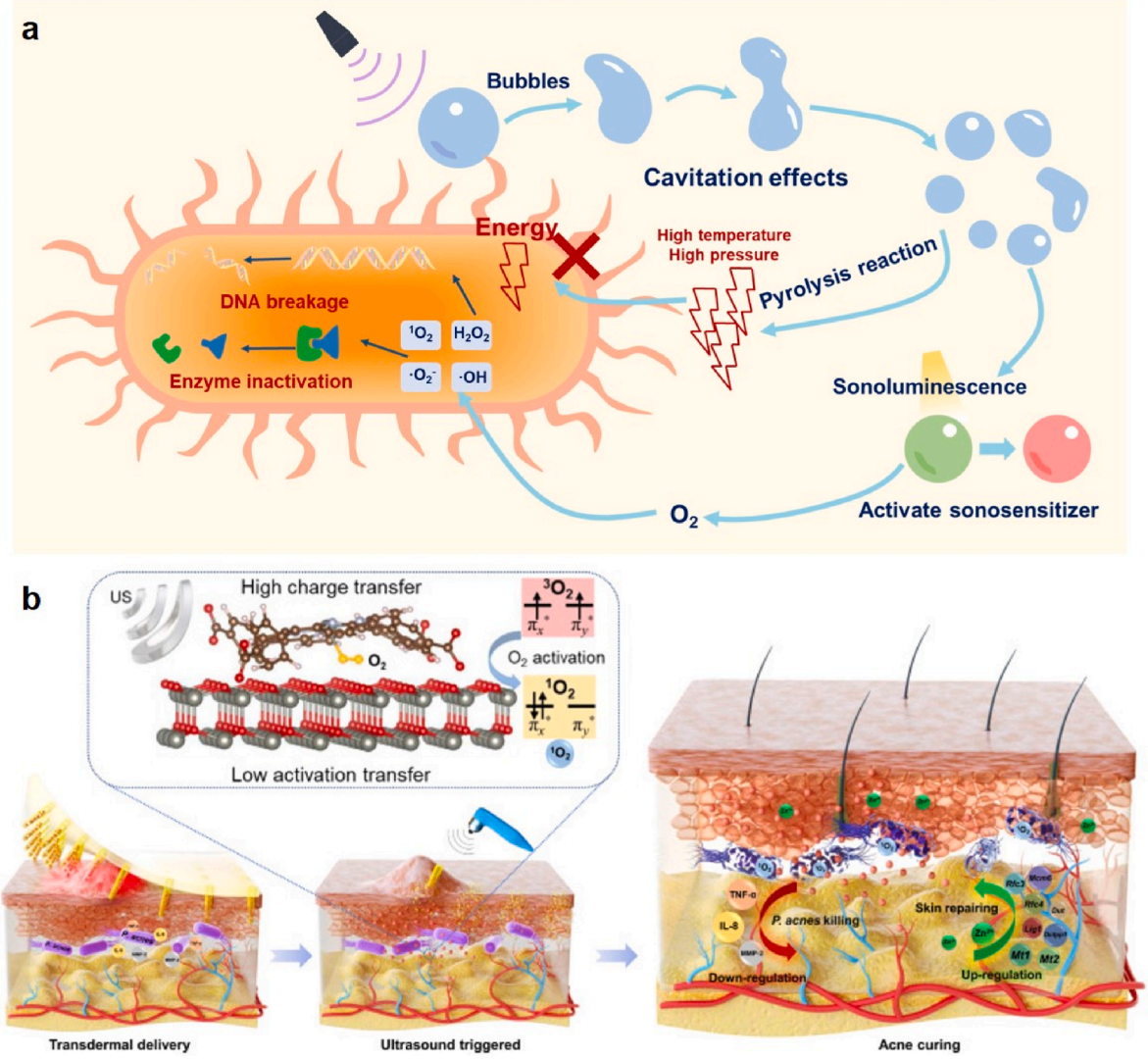

Fig. 11. SDT used for skin infections. **(a)** Antibacterial mechanism of SDT. **(b)** Schematic illustrating US-triggered and interfacial engineering-strengthened MN patch for topical acne treatment. Adapted from Ref. [26] with permission.

sonocatalytic properties of TiO_2 NPs with different phases for the first time. It was found that anatase–brookite TiO_2 exerted the highest antibacterial efficiency (99.94 %) against *S. aureus* after 15 min of US irradiation. Therefore, anatase–brookite TiO_2 was further delivered by HA MNs to the infected wound tissues. After the TiO_2-loaded MNs were applied to the wound, the deep-layered biofilms were effectively eliminated after 15 min of US irradiation, which further promoted wound healing. In another study, Liang et al. [104] developed CuO_2/TiO_2 integrated MNs to achieve sono-chemodynamically and sonothermally augmented antibacterial therapy. With the assistance of microneedle technology, CuO_2/TiO_2 NPs were delivered into deep dermis and activated by US to produce ROS and sonothermal effects, resulting in elimination of >99.9999 % multidrug resistant bacteria *in vitro* and *in vivo* within 5 min. These findings confirm the potential of non-antibiotic and sonosensitive therapies in infectious wounds.

MOFs have been extensively used in the biomedical field because of their special structure and photo/US-responsive nature. However, a single MOF has a poor US response owing to the rapid recombination of electron holes between its structures [26]. To improve the sonocatalytic performance of MOFs, researchers have attempted to modify the structure of these frameworks for guiding electron transfer and energy conversion. For instance, Xiang et al. [26] synthesized composite NPs containing zinc porphyrin-based MOF and ZnO (ZnTCPP@ZnO) to form an interface effect, which effectively enhanced the sonocatalytic performance and decreased the energy required for oxygen activation (Fig. 11b). The ZnTCPP@ZnO NPs were then loaded in HA MNs for topical treatment of acne (Fig. 11b). After 15 min of US irradiation, a large amount of ROS was produced to eradicate *P. acnes*, which resulted in a bactericidal rate of 99.73 % and a substantial decrease in the levels of acne-related factors. Moreover, Zn^{2+} released from the composite NPs up-regulated the DNA replication-related genes, further promoting the proliferation of fibroblasts and skin repair. Accordingly, the US-triggered MN patches with an interfacial engineered US response effectively treated acne infection.

2.6. Starvation therapy (ST)

ST, also known as starvation dieting, was first developed by the physician Frederick Allen to prolong the lives of patients with diabetes in the 1920s [105]. In 1971, ST was further proposed by Professor Folkman from Harvard University to treat malignant tumors, and the theory of ST is to cut off the nutrients supply to cancer cells [106]. Similar to tumor therapy, ST has also emerged as a novel antibacterial therapy, which consumes glucose to block the energy supply and proliferation of bacteria [107]. GOx is a commonly used biocatalyst in ST, which catalyzes glucose to decompose into gluconic acid and H_2O_2 under physiological conditions [108]. These decomposition products can be further used as substrates to sensitize other therapies for enhanced antibacterial performance. Particularly, H_2O_2 can be catalyzed by metal ions to produce ·OH with higher cytotoxicity, thus providing cascade treatment of ST and CDT. For instance, Zhao et al. [109] developed a cascaded nanocomposite consisting of apramycin, GOx nanocapsules (nGOx), and AgNPs for triple antibiotic/starvation/metal ion antibacterial therapy. When the nanocomposite was delivered to the infected skin site by MNs, it converted glucose into gluconic acid and H_2O_2 to accelerate the release of Ag^+ from AgNPs, resulting in significantly inhibited bacterial growth even at a low dose of antibiotics. With the removal of bacteria, the nanocomposite delivered by MNs promoted rapid scar-free skin recovery in both the *P. acnes*-infected mouse and rabbit models.

To prevent the inherent instability and rapid degradation of GOx in physiological conditions, some inorganic nanoenzymes with GOx-like activity have been proposed as a promising alternative for ST. For instance, Shan et al. [110] developed a catalytic MN patch loaded with NIR-II-responsive Au-Cu_2MoS_4 (Au-CMS) nanosheets for treating infectious diabetic wounds. The Au-CMS nanosheets had dual nanoenzyme activities of GOx and catalase, which simultaneously consumed local glucose to provide ST and catalyze the conversion of H_2O_2 into oxygen to facilitate the healing of diabetic wounds. In addition, the Au-CMS nanosheets exhibited excellent NIR-II photothermal property, enabling the synergism of ST and PTT to eliminate bacteria at the wound site. The Au-CMS integrated MN with excellent catalytic and photothermal properties produced robust antibacterial effects both *in vitro* and in MRSA-infected diabetic wounds, showing great potential for diabetic wound management.

2.7. Nanoenzyme antibacterial therapy (NABT)

The history of nanoenzyme research can date back to the late 20th century, when scientists began to focus on exploring the biocatalytic function of nanomaterials. In 2004, the term “nanoenzyme” was first proposed by Paolo Scrimin et al. [111] to describe the transphosphorylation reactivity of triazacyclononane functionalized gold NPs. In 2007, Yan et al. [112] reported the first discovery of Fe_3O_4 NPs with peroxidase-like activity, which is considered to be a pioneering study of nanoenzyme. In 2013, Wei and Wang further defined the concept of nanoenzyme as “nanomaterials with enzyme-like properties” in a review [113]. With the rapid development of nanotechnology, researches on multifunctional nanozyme-based therapy have made significant progress.

Benefiting from the multiple catalytic, antibacterial, and immunomodulatory activities of nanoenzymes, NABT has received increasing attention in treating skin infections, particularly refractory biofilm-infected or diabetic wounds [114,115]. Based on the catalytic activity, nanoenzymes are mainly divided into two types: (1) POD-like nanoenzymes, which can catalyze the decomposition of H_2O_2 into ·OH [116], and (2) the oxidase (OXD)-like nanoenzymes, which can catalyze the decomposition of O_2 into $\cdot O_2^-$ [117] (Fig. 12). The activity of nanoenzymes can be easily tuned and enhanced by introducing external stimuli, such as light [118], ultrasound [119], and metabolic regulator [12]). This enables nanoenzymes to provide multimodal anti-infection therapy by reshaping the hostile infectious, oxidative, and inflammatory microenvironment.

Biofilm infection, high glucose levels, and vascular blockages are the three major factors that hinder the healing of diabetic wounds. To remove these obstacles present in diabetic wounds, Yu et al. [15] reported a multi-enzyme cascade MN system that can hierarchically eradicate MRSA biofilms and promote angiogenesis. Specifically, α-amylase and GOx were loaded in MIL-101 NPs (MOF), followed by encapsulating in the needle of MNs for bacterial killing through vacuum casting. Methacrylic anhydride gelatin grafted with pro-angiogenic peptide (QHREDGS) was loaded in the base of MNs to promote tissue remodeling. After the MN patch was applied to the MRSA biofilm-infected diabetic wounds established in the mice, α-amylase was first released from the MNs to destroy the EPS surrounding the biofilm. Then, GOx consumed glucose in the wound to produce H_2O_2, which was further converted into ROS by the Fe^{3+} present in MIL-101 to eradicate bacteria encaged by the biofilm. With the decrease in tissue glucose and removal of bacteria, the inflammatory levels of wounds were decreased to promote wound healing. The QHREDGS-modified gelatin further promoted collagen deposition and vascular remodeling for accelerated wound healing. As a result, the infectious diabetic wounds were completely healed on day 12, demonstrating the great potential of MN multi-enzyme cascade activities in managing diabetic wounds.

The healing of skin wounds usually undergoes four stages, including hemostasis, inflammation, proliferation, and remodeling. In infectious chronic wounds, the proliferation of bacteria can cause persistent inflammation, making them difficult to heal [120]. To treat infectious chronic wounds, it should be better to eliminate bacteria and decrease inflammation levels involved in the wounds. However, there are spatiotemporal differences in the clearance of bacteria and inflammation. To meet the demands of wound healing in different stages, Shan

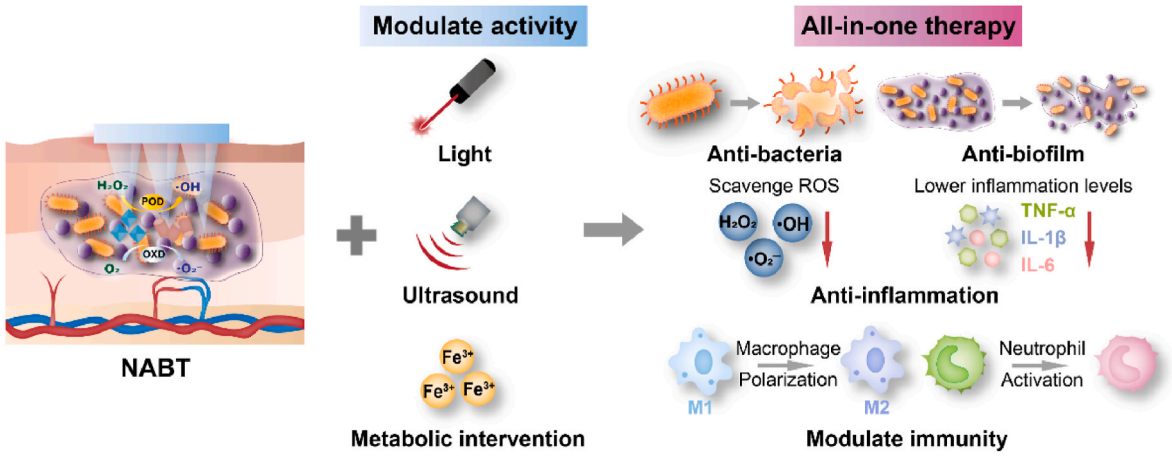

Fig. 12. Schematic illustration of NABT used as an "all-in-one" treatment strategy for skin bacterial infection. Based on the antibacterial mechanism, the nanoenzymes can be divided into POD-like and OXD-like ones. The activity of nanoenzymes can be modulated by introducing external stimuli (*e.g.*, light, ultrasound, metabolic regulator). Benefiting from the multiple antibacterial, anti-inflammatory, and immunomodulatory activities of nanoenzymes, NABT could provide an "all-in-one" therapy for skin infections.

et al. [121] designed spatiotemporal catalytic MN patches loaded with two antagonistic nanoenzymes (termed as CMSP-MNs) to treat infected wounds. In this study, Cu_2MoS_4 (CMS) NPs with POD-like catalytic activity were loaded in the tips to generate multiple ROS for bacterial killing in the infection stage. In contrast, PDA NPs with anti-inflammatory functions were loaded in the backing layers to eliminate over-produced ROS in the inflammatory phase. The CMSP-MNs displayed high bactericidal activity against MRSA and *E. coli in vitro*, eliminating 99.998 % of bacteria after 1 h of treatment. In addition, the CMSP-MNs effectively scavenged ROS (*e.g.*, H_2O_2, $O_2^{\bullet-}$, and •OH) and down-regulated the level of pro-inflammatory factors (*e.g.*, TNF-α, IL-6). Benefiting from their spatiotemporal adjustable catalytic performance, the CMSP-MNs accelerated the healing of MRSA-infected diabetic wounds and pressure ulcers established in mice, which reached about 95 % closure at day 12 and 100 % closure at day 6, respectively.

As most of the nanoenzymes used for antibacterial therapy largely depend on their POD-like activity, the local concentration of H_2O_2 may be a significant factor affecting the antibacterial effects of NABT [122]. However, the endogenous H_2O_2 in the diseased tissue is usually markedly limited. To produce sufficient ROS for efficient bacterial killing, the nanoenzymes are mainly integrated with exogenous H_2O_2 as a supplementation or endowed with additional GOx/GOx-like activity to convert glucose into H_2O_2 as a self-supply [115,123]. Recently, the OXD-like nanoenzymes that directly convert oxygen molecules into bactericidal ROS have captured increasing attention, as they can well address the problem of poor antibacterial effect caused by deficient H_2O_2 [124]. More attractively, the OXD-like nanoenzymes enable multimodal anti-infection therapy by introducing external stimuli such as electric field and light to modulate their catalytic reaction and activity. Shi et al. [125] recently developed HA MNs integrated with piezoelectric and photocatalytic nanoenzymes to provide antibacterial and anti-inflammatory combination therapy for MRSA-infected wounds. Briefly, graphitic carbon nitride (C_3N_5) nanosheets were first synthesized via a thermal polymerization approach, followed by decoration with platinum–ruthenium (PtRu) nanoalloys to construct multifunctional nanoenzymes (PtRu/C_3N_5). Under the US, PtRu/C_3N_5 showed piezoelectric-enhanced OXD-like activity, which was 3.9-fold higher than that of C_3N_5. After ultrasound for 10 min, PtRu/C_3N_5 showed a broad-spectrum antibacterial effect and killed almost 100 % of the bacteria *in vitro* and *in vivo*. The PtRu nanoalloys with photocatalytic activity triggered the production of H_2 gas upon visible light irradiation to reduce inflammation levels and accelerate infectious wound healing. Benefiting from the piezoelectric and photocatalytic activities of PtRu/C_3N_5, the PtRu/C_3N_5-loaded MNs offered an "all-in-one" antibacterial and anti-inflammatory therapy for infectious wounds.

In addition to the conventional treatment modalities mentioned above, iron-based nanoenzymes that can interfere the bacterial metabolism and immune cell functions have also been proposed to treat refractory bacterial infection. Zhao et al. [12] developed MN patches integrated with Fe_3O_4-based photothermal nanoenzyme to provide iron-actuated Janus ion therapy (IJIT) for refractory biofilm-induced infection. Briefly, Fe_3O_4-dopped graphene oxide (FGO) nanosheets were loaded in MeHA gel to fabricate photothermal MN patches (FGO@MN) that could respond to the biofilm infection microenvironment. FGO not only catalyzes the conversion of H_2O_2 into ·OH but also sensitizes the biofilm to PTT by destructing the heat-shock proteins in bacteria. Further, FGO, with excellent photothermal performance, produced a mild photothermal treatment to trigger intracellular uptake and overload of iron, which finally caused the biofilms to undergo ferroptosis-like death. Meanwhile, the neutrophils in the biofilm infection microenvironment acquired iron as a nutrient, rejuvenating and reactivating their ability to suppress the growth of biofilms. More than 95 % of biofilms were eliminated by integrating iron-sensitized PTT, iron-induced ferroptosis-like death, and iron-nourished immune reactivation. After treatment with FGO@MN for 15 days, refractory bacterial biofilm-induced infections were scavenged in biofilm-implanted mice and wound-bearing diabetic mice, suggesting that IJIT has good prospects for clinical application.

2.8. PIL-based therapy

In recent years, ionic liquid (IL) has been exploited as a novel antibacterial agent to overcome antibiotic resistance. IL usually refers to salts that consist of definite anions and cations and have a melting point below 100 °C [126]. PIL is defined as a class of polymers made from IL monomers with highly stable physicochemical properties. Both IL and PIL have unique antibacterial mechanism and broad-spectrum antibacterial activity. The functional cationic groups present in IL or PIL, such as imidazolium, pyrrolidinium, and quaternary ammonium, form electrostatic interaction with negatively charged bacterial cell walls, and their lipophilic alkyl chains further destroy the bacterial cell membrane via hydrophobic interaction [127,128]. The combination of cationic PIL and anionic active via electrostatic interaction could be constructed as a multifunctional drug delivery system for better therapeutic outcomes. For instance, Zhang et al. [129] developed salicylic acid (SA)-loaded PIL-based MNs for enhanced treatment of acne infections. The PIL-based MNs were prepared by photo-crosslinking of an imidazolium-type IL monomer in the micro-molds of MNs, followed by anion exchange with

SA^-. The PIL-based MNs exerted excellent antibacterial activity against *E. coli*, *S. aureus*, and *P. acnes* and efficiently decreased the levels of proinflammatory cells and cytokines (TNF-α and IL-8) in the *P. acnes*-infected mice model, showing great potential for treating skin acne infections. In another study, Chao et al. [130] prepared four kinds of imidazole IL-based MNs and studied the effect of the carbon chain lengths of IL monomers on their antibacterial performance. It was found that the increase in substituent carbon chain lengths contributed to improved antibacterial activity. Moreover, the IL-based MNs enabled self-sterilization of the administration site, where tiny holes were created after the insertion of MNs into the skin.

In summary, antibacterial MNs have achieved great success in the treatment of skin infections. Researchers have made great efforts to exploit novel antibacterial agents or therapies (*e.g.*, antimicrobial peptide, PTT, PDT, MABT, CDT, SDT, ST, PIL) to effectively combat biofilm-induced skin infections. These innovative antibacterial therapies can increase the permeation of the drug into the biofilm by destroying the bioactive components of the biofilm. Benefiting from their multitarget antimicrobial effects, they can be used as potential substitutes for antibiotics to avoid the emergence of multidrug-resistant bacteria. Furthermore, some promising strategies have been proposed to improve the antibacterial effect of MNs: (1) The geometrics and components of MNs are key factors affecting their mechanical properties and drug delivery efficiency. For instance, cone MNs was reported to show better mechanical properties and skin insertion ability than cone-cylinder, hexagonal pyramid, and rectangular pyramid MNs [131]. In addition, the introduction of hyaluronidase to MNs was reported to enhance the mechanical strength and drug transdermal permeability of MNs, resulting in higher drug retention in the lesional skin tissues [132]. Therefore, optimization of microneedle geometrics and components may provide an easy approach to increase the antibacterial effect of MNs. (2) Harnessing the physicochemical source originating from α-amylase, light, ultrasound, or nanomotor to break through the barrier of biofilm for deeper drug penetration and more efficient bacterial removal; (3) Developing combination therapies to initiate complementary bacteria killing mechanisms. With a deeper understanding of the pathogenesis and pathological characteristics related to skin infections, all-in-one therapy (*e.g.*, NABT, IJIT) that integrates antibacterial, anti-inflammatory, and immunomodulatory activities comes to revolutionize the treatment of skin infections, particularly chronic wound infections.

3. MNs used to treat fungal infections

Fungal infections are usually more difficult to treat than bacterial infections, because eukaryotes have thicker and more rigid cell walls to protect the fungi from lysis by the host immune system [133]. It is estimated that there are approximately 1 billion people experiencing fungal infection and more than 1.5 million deaths worldwide annually [134]. Superficial fungal infection can lead to a series of dermatomycosis, which may occur on the hands, feet, or toenails, and is usually treated by oral or transdermal administration of antifungal medicines. However, deep fungal infection, such as SSTI, has become a thorny medical problem, as it can cause serious sequela, especially for immunocompromised populations, such as patients with AIDS, cancer, and malnutrition [135]. Oral or injectable administration of antibiotics is the common approach used to treat deep fungal infections, while their therapeutic effects are far from satisfaction even with repetitive dosing. A promising alternative for treating cutaneous fungal infections topically is the use of MNs, which have recently emerged and offer improved therapeutic efficiency.

3.1. Drug therapy

Drug therapy is the first-line therapy for skin fungal infections. In 2013, Boehm et al. [136] prepared antifungal MNs for the first time. In this study, they used piezoelectric inkjet printing technology to prepare coated MNs by depositing amphotericin B (AmB) solution onto the surface of biodegradable Gantrez AN 169 BF needles. The agar plate test demonstrated that AmB-coated MNs exerted certain antifungal activity against *Candida parapsilosis*. Therefore, the MN-mediated intradermal delivery of antifungal actives shows great potential for treating cutaneous fungal infections. However, the commonly used antifungal drugs, such as AmB and itraconazole (ITZ), are poorly water-soluble. The development of antifungal dissolving MNs, therefore, yields the problems of poor drug solubility and low drug loading. Engineering of these insoluble drugs into nanomedicines is a common approach to simultaneously improve the drug solubility and loading capacity of MNs [137]. In the study by Nasiri et al. [138], AmB was first formulated into nanoemulsion via a probe-sonication method, followed by loading in dissolving MNs for enhanced intradermal drug delivery. The transdermal permeation studies on the excised porcine skin revealed that the emulsion-based MNs showed about a five-fold increase in the cumulative permeability of AmB as compared with AmB-loaded emulsion. Further, the Capmul MCM C-8 EP/NF used for the preparation of the nanoemulsion showed synergistic antifungal activity with AmB against *C. albicans*. In the study by Permana et al. [139], ITZ nanocrystals-incorporated dissolving MNs were devised for improved treatment of cutaneous candidiasis. A media milling technology was used to prepare the ITZ nanocrystals, and Pluronic®F127 was used as a stabilizer to improve the stability of these ITZ nanocrystals. Compared with the ITZ crude dispersant, ITZ nanocrystals showed a three-fold increase in the drug dissolution rate and a 1000-fold increase in the antifungal activity, resulting in the complete elimination of *C. albicans* after 48 h of administration.

Enlightened by the success of MNs for cutaneous fungal infection, researchers have been devoted to improving the therapeutic efficacy of MNs through intelligent design. For instance, Peng et al. [140] developed novel hybrid MNs consisting of AmB-loaded PLGA tips and a hydrogel baseplate for treating *C. albicans*-induced infection. The alternative of hydrogel baseplate to conventional soluble baseplate made it easier for MNs to peel off from the skin and successfully sped up the implantation of the PLGA tips into the skin. As a result, the drug delivery efficiency of MNs is increased by up to 80 %. The disk diffusion test showed that the optimized hybrid MNs inhibited the growth of *C. albicans*, while the PLGA tips yielded continuous release of AmB for a week and hence long-acting treatment of cutaneous fungal infections.

3.2. Novel therapies

Except for the antifungal chemicals, researchers have developed some novel and efficient therapies (*e.g.*, nanoenzyme, antimicrobial peptides, living bacteria, and gas therapy) to treat intractable fungal infections, such as deep cutaneous fungal infections (DCFI) and SSTI. Detailed examples are shown below.

3.2.1. Combination of nanoenzyme and antimicrobial peptide

Rapid development of drug resistance is a common problem in skin infections, which eventually leads to the failure of treatments. It has become the incessant pursuit of researchers to prevent microbial drug resistance. To combat the drug-resistant fungi, Wang et al. [141] developed copper sulfide (CuS) nanoenzyme and antimicrobial peptide (PAF-26) co-loaded MNs (CuS/PAF-26 MNs) for the combination treatment of DCFI (Fig. 13a). The CuS nanoenzyme with dual OXD-like and POD-like activities catalyzed H_2O_2 to generate ROS, while PAF-26 immediately destroyed the cell envelop of fungus and further assisted in the penetration of CuS-generated ROS to the fungus for better antifungal effects. The combination of CuS with PAF-26 yielded excellent synergistic antifungal activities against *C. albicans in vitro* (Fig. 13b–d), and their resultant MIC value remained unchanged even after culturing the *C. albicans* for six passages, thus preventing the potential fungal drug resistance. The pharmacodynamics studies on the *C. albicans*-inoculated

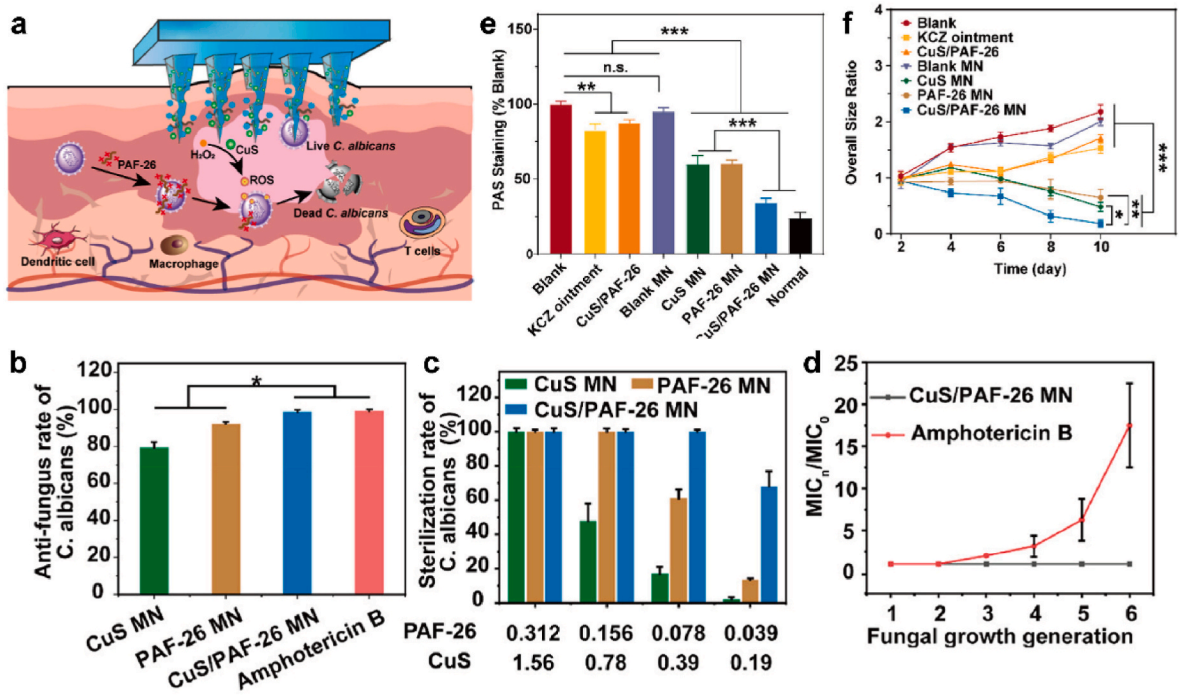

Fig. 13. MN-mediated codelivery of nanoenzyme and antimicrobial peptide for combined treatment of DCFI. **(a)** Schematic illustration of CuS/PAF-26 MNs to treat DCFI. *In vitro* antifungal activity: **(b)** Representative images and **(c)** quantitative analysis of *C. albicans* colonies treated with different agents, **(d)** Antifungal rate of different treatments against *C. albicans*, **(e)** Changes in drug resistance of *C. albicans* after treatment with CuS/PAF-26 MN and amphotericin. The therapeutic efficacy of CuS/PAF-26 MNs to treat DCFI: **(f)** Periodic Acid-Schiff (PAS) staining percentage of different treatment groups versus the control group to demonstrate the *in vivo* antifungal activity, **(g)** Change of the fungal infected nodule sizes (normalized to the initial size) after different treatments. Adapted from Ref. [141] with permission.

mouse model further demonstrated that the CuS/PAF-26 MNs were most effective in eradicating *C. albicans* (Fig. 13e) and decreasing the size of the nodules (Fig. 13f). These encouraging results collectively demonstrated the great potential of CuS/PAF-26 MNs to treat DCFIs.

3.2.2. Living bacteria

Given the natural competition law, some dominant bacteria have been increasingly explored as natural antimicrobial agents against diverse infections [142]. The main antifungal mechanism of these bacteria is to secrete antifungal agents such as lipopeptides (LPS) and destroy the cell membrane for fungal killing, which makes them capable of reducing fungal resistance and preventing drug-related adverse reactions [143,144]. By virtue of the unique antifungal mechanism of dominant bacteria, Wang et al. [145] developed living MNs (LMNs) loaded with functionalized active *Bacillus subtilis* for treating cutaneous fungal infection. For the preparation of the LMNs, *B. subtilis* was evenly dispersed in a mixed solution of poly (ethylene glycol) diacrylate (PEGDA) and PVA, followed by solidification under ultraviolet (UV) light irradiation. The activity of *B. subtilis* was well maintained in the LMNs, as evidenced by the green dots observed from the immunofluorescence images. After the LMNs were inserted into the skin, PVA absorbed tissue interstitial fluid and dissolved, forming pores in the photo-crosslinked hydrogel MNs. The resultant pores enabled the bacteria to absorb body nutrients and maintained the activity of the bacteria, while the encapsulation of the bacteria into the MNs protected them from attacks by the host immune system. Accordingly, the living bacteria continuously produced multiple antifungal agents to kill *C. albicans*, resulting in significantly higher antifungal performance *in vitro* and *in vivo* than ketoconazole. Moreover, the bacteria were eliminated along with the MNs, thus reducing the potential risk of bacterial infection and related concomitant syndrome. Notably, the delivery efficiency of the antifungal agents to the infected site was improved to obtain better therapeutic outcomes by adjusting the height of the MNs to accommodate the depth of infection. These positive results show the great potential of LMNs for treating cutaneous fungal infections.

3.2.3. NO-based gas therapy

NO-based gas therapy has been investigated as a potential substitute for traditional antibiotics to treat microbial infection, owing to its unique antimicrobial mechanism and distinct merits [146]. When NO is present in aerobic conditions, it can react with ROS to generate more oxidative reactive nitrogen species (RNS) (*e.g.*, N_2O_3, $ONOO^-$, $NO_2\bullet$). These RNS can cause damage to metabolic enzymes, microbial cell membranes, DNA, and proteins through nitrosative or oxidative processes. Chemical damage of DNA by RNS is regarded as the main antimicrobial mechanism of NO, as it can disrupt the intact microbial membrane and cell functions to induce microbial death [146]. NO can exert broad-spectrum antimicrobial activities without drug resistance are exerted by due to its unique antimicrobial action against bacteria, fungi, and biofilm. NO can also sensitize other antimicrobial treatments (*e.g.*, PTT [147], PDT [148], CDT [149], antibiotics [150]) to improve therapeutic outcomes. Owing to the extremely short half-life (<5 s) and high reactivity of NO *in vivo*, it is difficult to control the release of NO at a proper rate for an extended period [151]. To overcome the inherent shortcomings of NO, researchers have developed several types of NO donors with NO-releasing capability, including nitrates, N-diazeniumdiolates (NONOates), and S-nitrosothiols (RSNOs). However, these conventional NO donors require strict trigger conditions (*e.g.*, light, enzyme, ions) to release NO and yield safety problems. Given that the local delivery of NO to the infection site could shorten the diffusion distance of NO and increase the therapeutic efficacy, Zhang et al. first devised NO-releasing PIL-based MNs (PILMN-NO) for topical treatment of *C. albicans*-induced SSTIs (Fig. 14) [152]. Briefly, imidazole-type PIL was generated and then used to produce PIL-NONOates through the chemical reaction between $-NH_2$ in 3-(2-hydroxyethyl)-1-vinylimidazolium 3-amino-1-propanesulfonic acid (HEIm) and NO. After that, PILMN-NO was obtained by photocrosslinking of the MN components under 365 nm UV irradiation for 30 min. NO was

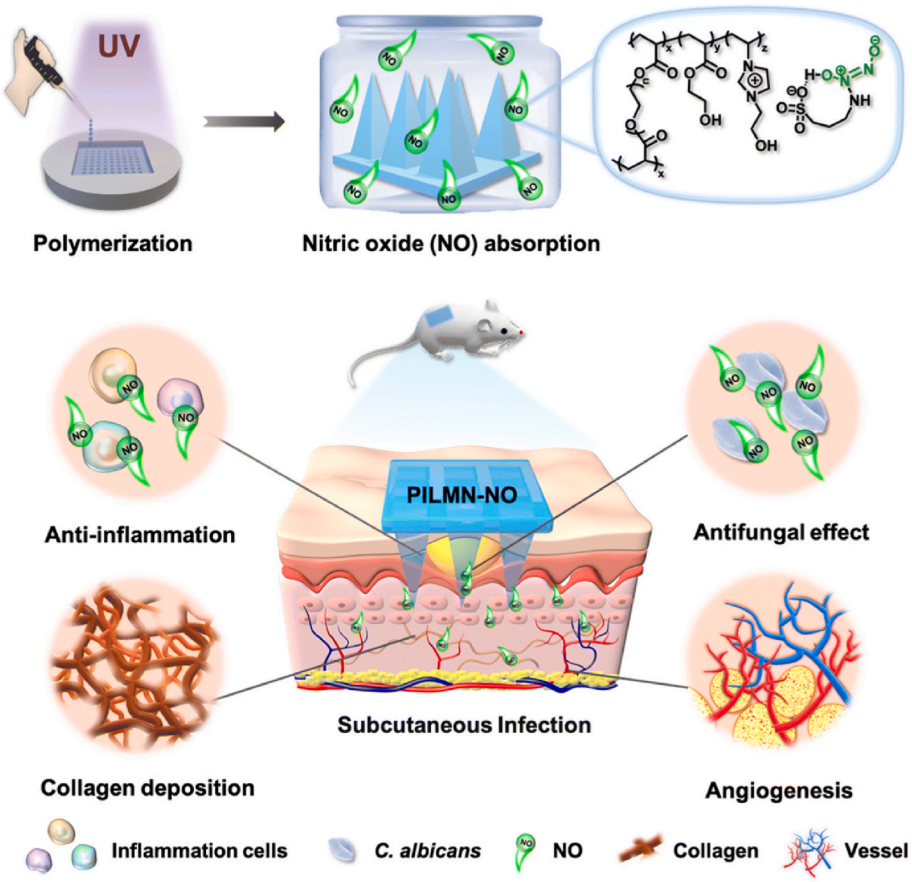

Fig. 14. Schematic illustration of PILMN-NO MN for treating deep skin fungal infection through the multiple actions of fungal killing, antiinflammation, and angiogenesis. Adapted from Ref. [152] with permission.

readily released from PILMN-NO under physiological conditions and synergized with PIL to eliminate *C. albicans* and its biofilm both *in vitro* and *in vivo*. As expected, accelerated wound healing could be observed with increasing release of NO, as NO effectively suppresses inflammatory reaction, promotes angiogenesis, and facilitates collagen synthesis. Accordingly, infected wounds were almost completely healed after 11 days of treatments. These positive results demonstrated the potential of PILMN-NO for treating deep skin fungal infections.

4. MNs used to treat viral infections

Viral skin infections can cause various skin diseases, including herpes simplex, warts, varicella, herpes zoster, or measles. The emergence of antiviral MNs enables topical treatments of viral skin infections with improved patient compliance and therapeutic efficiency. The recent application of antiviral MNs is mainly centered on herpes and warts and described as below.

4.1. Drug therapy for herpes

Herpes labialis, also known as cold sores, is a common herpes simplex that occurs on the lips and is particularly caused by herpes simplex virus-1 (HSV-1) [153]. Acyclovir is the only definitive therapeutic drug for the treatment of herpes labialis. However, acyclovir belongs to the BCS Class III drug class and has poor skin permeability, making it difficult for transdermal administration of acyclovir to obtain satisfactory clinical benefits even after long-term treatment. Further, conventional transdermal preparations have limitations in delivering acyclovir to the deepest epidermal layers, where HSV-1 is commonly replicated. Microneedle technology has been proved to provide target delivery of acyclovir with enhanced delivery efficiency. For example, Yan et al. [154] developed solid silicon MNs with various needle lengths and needle densities for intradermal delivery of acyclovir and evaluated the influence of geometric parameters on drug efflux. The results revealed that MNs with a needle length exceeding 600 μm and a needle density less than 2000 needles/cm^2 had higher drug efflux, as they can more efficiently decrease skin electric resistance and create drug delivery pathways. In a further study, Pamornpathomkul et al. [155] devised dissolving MNs to improve the transdermal delivery efficiency of acyclovir. Compared with Lipsore®, a commercial cream, MNs showed an approximately 45-fold increase in the percentage of acyclovir permeating across the skin and a 16-fold increase in drug accumulation in the basal epidermis. In addition, MNs prolonged the retention time of acyclovir in the target skin layer, as evidenced with about 75 % of delivered drug retained for 48 h. These findings suggest that MNs are a promising alternative to commercial creams for enhancing therapeutic efficacy.

4.2. Drug therapy for warts

Warts are common skin lesions caused by human papillomavirus (HPV), which mainly proliferates in the granular skin layer of the epidermis. The emergence of warts can lead to epidermal hyperplasia and hyperkeratosis, which can have a negative impact on the overall quality of life for patients owing to physical discomfort and increased self-consciousness [156]. In appearance, warts manifest as plaques of various sizes and rough scaly surfaces that may spread on the hands or soles of the feet [157]. Warts occur particularly in children at an incidence of approximately 10 %. The major types of nongenital warts are common warts, plantar warts, and flat warts. The primary treatments

used for warts are broadly classified into aggressive therapies (*e.g.*, cryotherapy, excision, laser ablation, electrocautery) and topical therapies (*e.g.*, bleomycin injections, topical imiquimod, topical salicylic acid) [156]. Topical therapies are more tolerated by patients but require more treatment sessions than aggressive therapies. The hyper-keratinized epidermis noted in patients with warts is remarkably thicker and harder than the normal skin, making it difficult for topical agents to reach the lesion site. Additionally, intralesional injection yields unavoidable problems of drug leakage, inaccurate injection depth, and marked pain, resulting in poor therapeutic outcomes. In view of these dilemmas, MN-mediated or MN-assisted topical drug delivery may serve as a better therapeutic option for warts, as therapeutic agents could be easily delivered to the subepidermal skin layer with high efficiency, further reducing the dosing frequency.

In the past decade, both preclinical and clinical tests have demonstrated that MNs have the potential to improve the therapeutic efficiency of warts. For instance, Lee et al. [158] used a dip coating technology to devise bleomycin-coated MNs to treat warts. The amount of bleomycin delivered into the skin increased with growing insertion time and reached a peak value (82 %) after 15 min of insertion. Compared with intralesional injection, the bleomycin-coated MNs remarkably prolonged the residence time of bleomycin in the subepidermal skin layer based on drug distribution and pharmacokinetic studies. These data indicate that MNs provide a potential target therapy for warts. In other studies, several clinical trials demonstrated the potential benefits of MNs in treating warts [153,159,160]. In general, MNs performed similarly to conventional cryotherapy in clearing warts but eliminated the intense pain caused by cryotherapy or injection. Further, MNs increased the delivery efficiency of loaded drugs or other drug formulations. These positive outcomes indicate that MNs hold great potential for enhanced topical treatment of warts.

5. MNs used to detect skin infections

The proposal of precision medicine indicates that human medicine has entered a new era. To realize precision medicine for effective and on-demand treatment, current studies have centered on devising biosensing MN patches to recognize specific pathogens [20], track the status of infection [161], and monitor the therapeutic drug concentration in real time [23].

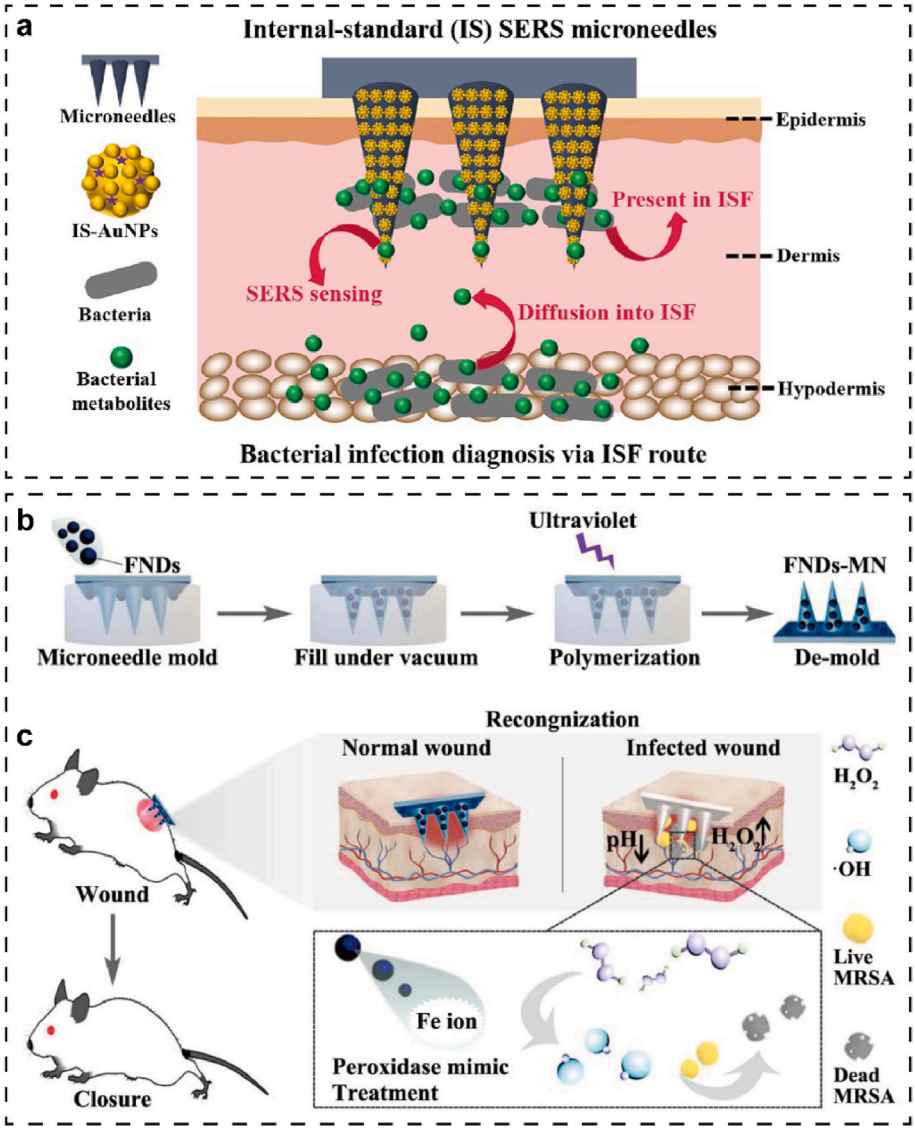

Fig. 15. MNs used for the diagnosis and treatment of skin infections. **(a)** Schematic illustration of IS-SERS-MNs integrated with surface-enhanced Raman scattering technique for bacterial infection diagnosis via ISF route. Adapted from Ref. [20] with permission. **(b)** Preparation and **(c)** therapeutic mechanism of FNDs-loaded MNs for MRSA-infected wounds. Adapted from Ref. [161] with permission.

5.1. Biosensing MNs used to diagnose microbial infections

Precise diagnosis of infectious pathogens is crucial for treating skin infections. Recently, minimally invasive detection of bacterial metabolites in skin ISF as biomarkers has emerged as a promising candidate for diagnosing infections since the compositions of ISF are highly correlated with those of blood [162,163]. MNs have been increasingly implicated as a powerful tool for collecting and detecting biomarkers in ISF derived from the epidermis and dermis [25,164]. Compared with blood analyses, biosensing methods avoid the complex process of sample extraction, separation, and analysis, thus offering a more convenient point-of-care testing (POCT) diagnostic approach. However, MN-assisted ISF-based biosensing is confronted with two major challenges, including complicated and time-consuming detection procedures and a lack of suitable biomarkers and biosensing techniques. To address these two challenges, Mei et al. [20] first developed highly sensitive biosensing MNs (IS-SERS-MNs) integrated with internal-standard surface-enhanced Raman scattering technique to detect bacterial metabolites as biomarkers of infection (Fig. 15a). The IS-SERS-MNs were prepared by the in situ growth of internal-standard embedded AuNPs on the surface of poly (methyl methacrylate) (PMMA) MNs. Pyocyanin is selected as the biomarker of *P. aeruginosa* infection, since it is the representative metabolite of *P. aeruginosa*. The sensitivity of the IS-SERS-MNs to detect pyocyanin in ISF was evaluated by using pyocyanin-loaded agarose hydrogels and living mouse as the simulated dermis and animal models, respectively. The sensitivity of the IS-SERS-MNs in detecting the ISF-derived pyocyanin from the living mouse reached a micromolar level, which was confirmed in the following three conditions: (1) detecting the release of pyocyanin from MNs in the dermis, (2) detecting the diffusion of pyocyanin to the dermis by injecting *P. aeruginosa* to the hypodermis, and (3) detecting dermal pyocyanin in the *P. aeruginosa*-infected mouse wounds. Pyocyanin was clearly detected at 24 h of infection, and the highest SERS intensity was obtained at 48 h to indicate the proliferation of *P. aeruginosa* at the wound site. These data collectively confirm the potential of IS-SERS-MNs as a minimally invasive and painless approach for diagnosing skin infections.

5.2. Colorimetric MNs used to report the status of infection

It is widely acknowledged that the microenvironment of infected tissue differs from that of normal tissue regarding the pH and ROS levels. Therefore, the detection of the changes in pH and H_2O_2 levels is a feasible approach for evaluating the progression of skin infections. For instance, Shan et al. [161] developed colorimetric MN patches that could undergo color changes as a response to the pH and H_2O_2 levels in order to intelligently manage infectious wounds. The colorimetric MN patches were prepared by loading Fe ion–gallic acid coordination polymer nanodots (FNDs) inside the MNs using a vacuum-based microperfusion method, followed by curing under UV light irradiation for 15 s (Fig. 15b). The POD-like activity of FNDs was pH-dependent, which enabled the conversion of H_2O_2 into a larger amount of •OH in the acidic microenvironment for superior antibacterial effects. During the treatment of wounds infected with MRSA in mice, the color of the colorimetric MNs changed with the status of infection, thus guiding the on-demand treatment of infectious wounds (Fig. 15c).

5.3. Biosensing MNs used to monitor therapeutic drugs

Antibiotics are clinically used as the golden-standard antimicrobial therapy for treating skin infections; however, their pharmacokinetics following existing treatment practices vary greatly among patients. It is estimated that up to 50 % of all antibiotics prescribed to humans are unnecessary and at least 50 % of antibiotic treatments are ineffective [165]. In addition to improving clinical outcomes, individualized antibiotic dosing minimizes adverse effects such as toxicity and microbial resistance [166]. These evidences highlight the importance of therapeutic drug monitoring (TDM) in guiding individualized antibiotic dosing. During treatment, discrete blood analysis and microdialysis are two common approaches used to monitor antibiotic concentrations. However, implementing these approaches is usually a complicated process, making them present operational, technical, and temporal challenges. The standard practices for conventional TDM include blood or extracellular fluid sampling, sample pretreatment, and drug analysis via chromatography and immunoassay (Fig. 16a). Such tedious procedures are labor-intensive and time-consuming, greatly restricting the temporal resolution of obtained pharmacokinetic parameters. TDM may not be useful in optimizing antibiotic dosing owing to the lag time in capturing pharmacokinetic information. To circumvent these dilemmas, researchers have proposed MN-based biosensing techniques as a promising alternative to realize real-time monitoring of antibiotic concentration.

β-lactam antibiotics have been widely used to treat infectious diseases; however, they have a high incidence of developing bacterial resistance. Real-time monitoring of the pharmacokinetics of β-lactam is critical for guiding rational dosing and reducing bacterial resistance. Recently, Gowers et al. reported the use of an MN-based sensor to continuously detect the concentration of β-lactam antibiotics *in vivo*. The MN-based sensor was coated with iridium oxide as a pH-sensing layer for the detection of the local changes in pH level caused by the β-lactamase-induced hydrolysis of β-lactam antibiotics. Through optimization of the biosensor coatings, the MN-based sensor yielded a detection limit of 6.8 μM penicillin in 10 mM PBS solution and real-time detected the concentration of penicillin in dialysate and serum. After sterilization and application for 6 h, the MN-based sensor could still retain its sensitivity. These positive results demonstrate the potential of MN-based sensors for real-time monitoring of antibiotic concentration and further personalized therapy. In 2019, Rawson et al. [24] conducted the first-in-human study of MN-based sensors for monitoring the concentration of phenoxymethylpenicillin in extracellular fluid. The results obtained from the MN-based sensor were consistent with those from standard microdialysis. In the follow-up study, Lin et al. [23] reported the use of a wearable MN-based electrochemical aptamer biosensor (μNEAB-patch) to provide real-time measurement of antibiotics with narrow therapeutic windows (Fig. 16b–d). Ag NPs were coated on the surface of MNs using a one-step deposition approach to serve as the working electrode and shield the interference peaks of nickel, thus rendering a high-quality surface to bind aptamer and improving the signal-to-noise ratio (SNR) of the MN-based biosensor. The pharmacokinetic studies on Sprague-Dawley rats confirmed the ability of the μNEAB-patch to track the ISF pharmacokinetic profile of tobramycin and vancomycin. The drug levels in ISF and circulation showed a high correlation and was linearly proportional to the administered dosage. These results collectively demonstrate the potential of μNEAB-patches for timely predicting total drug exposure and guiding rational antibiotic dosing.

6. Limitations of MNs used to treat and detect skin infections

The safety of antimicrobial MNs in terms of their administration, pharmacokinetics, and pharmacodynamics should be a paramount concern when transitioning them from laboratory settings to practical applications. Although MNs offer numerous benefits in the treatment of skin infections, researchers continue to face challenges due to certain adverse effects associated with MN administration (Fig. 17a). These adverse effects include but are not limited to infection, irritation, hyperpigmentation, contact dermatitis, and granulomas. Fortunately, the occurrence of these unfavorable incidents is typically infrequent and can be resolved without external intervention within a few hours to several days. Moreover, even with repeated use of MNs, the likelihood of infection resulting from microbial invasion through the MN-induced micropores is generally lower than that caused by hypodermic injections [167,168]. It is worth noting that polymeric MNs, which can

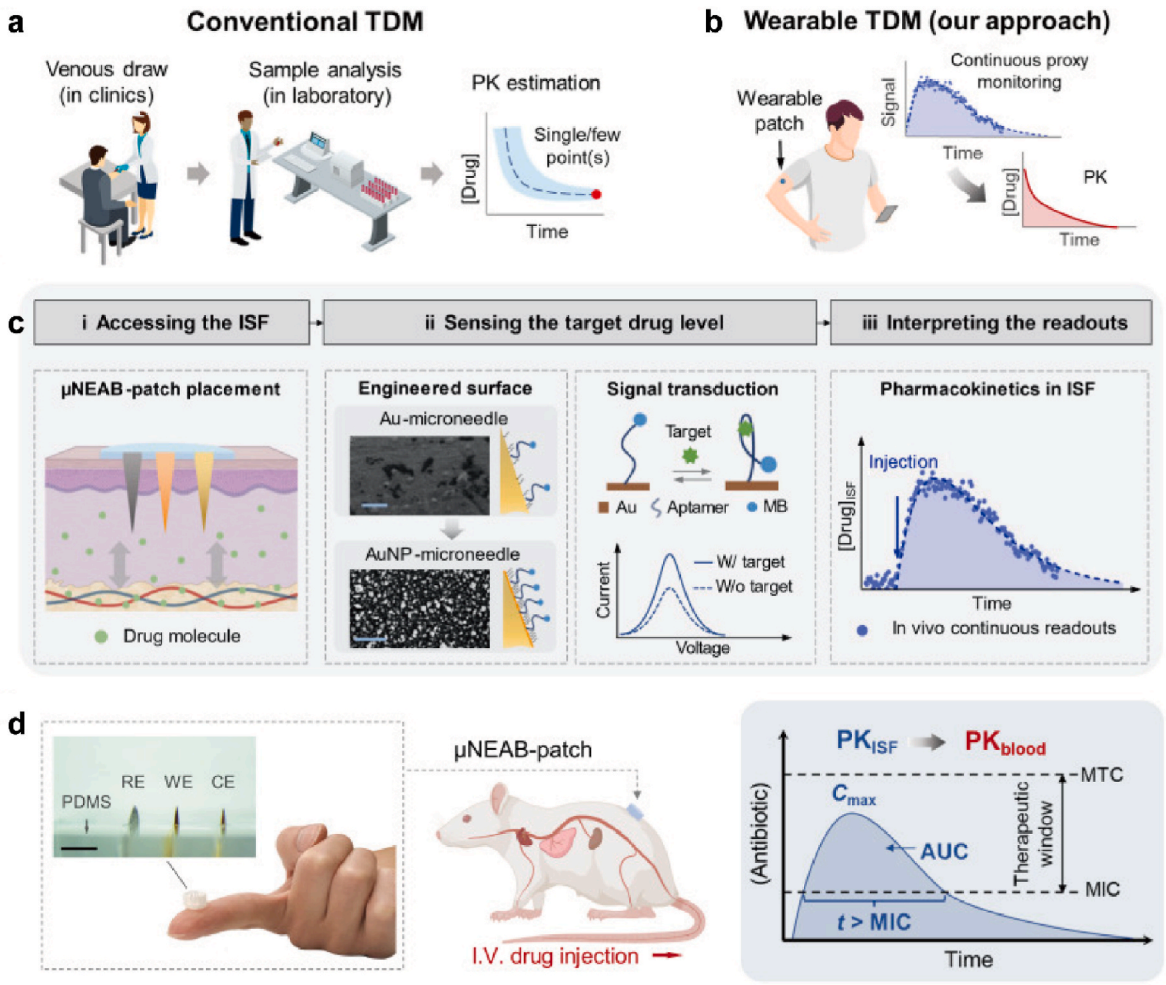

Fig. 16. Development of biosensing MNs for real-time monitoring of antibiotic pharmacokinetics. The procedures involved in **(a)** conventional TDM and **(b)** wearable TDM. **(c)** The process of μNEAB-patch used to real-time track the pharmacokinetics of antibiotics in ISF. **(d)** Schematic illustration of using μNEAB-patch to conduct TDM in a rat model.

dissolve within the skin without leaving sharp tips behind, effectively mitigate the risk of skin irritation and the potential for cross-contamination inherent in solid, coated, and hollow MNs [169]. This type of infection can be efficiently prevented by cleansing the application site with a 70 % isopropanol solution prior to administration. Additionally, it is imperative to maintain sterility when utilizing antimicrobial MNs for the treatment of skin infections. To mitigate the risk of deformation or dissolution of polymeric MNs caused by conventional sterilization techniques such as dry heat, steam sterilization, and microwave, gamma radiation sterilization or aseptic manufacture can be employed for polymeric antimicrobial MNs to prevent potential infection [170,171]. However, implementing these operations typically incurs high costs and complexity, thereby increasing the overall production expenses for enterprises. Consequently, it is crucial to explore more cost-effective methodologies to enhance the safety of antimicrobial MNs.

Maintaining consistent pharmacokinetics among patients is another problem that could not be well resolved in the current stage (Fig. 17b). This lack of consistency in pharmacokinetics is a significant obstacle to the clinical implementation of MNs, as evidenced by the withdrawal of M207 (developed by Zosano Pharma to treat migraine) from Phase III clinical trial [172]. The pharmacokinetics of drugs administered through MNs can be influenced by factors such as variations in the dose accuracy and efficiency of drug delivery. Due to the unavoidable variation in skin thickness among individuals and body locations, the skin insertion depth of MNs may vary from person to person and from site to site, making it difficult to achieve consistent delivery dose. Furthermore, the skin pores formed by MN puncture are prone to closure during administration due to their dynamic recovery process, thereby hindering the delivery of partial drugs to the cutaneous tissue [173]. This case is a prevalent occurrence in solid microneedles (MNs), wherein drugs are typically administered post-insertion of MNs into the skin to create microchannels [174]. It is important to acknowledge that the cargoes loaded in the coating layer of coated MNs may be exfoliated from the skin surface during administration [175]. Additionally, the resilient properties of the skin may impede MN puncturing, resulting in incomplete puncture and the presence of drug remnants on the skin surface. If the drug loaded in the MNs was not completely delivered to the cutaneous tissue, the drug delivery dose accuracy of MNs will be compromised, resulting in pharmacokinetic inconsistencies among patients. Currently, several approaches have been proposed to improve the pharmacokinetic consistency of MNs. One feasible approach is to increase the mechanical strength of polymeric MNs by some physical (*e.g.*, using composite materials with complementary properties) or chemical (*e.g.*, photo or ionic cross-linking of polymers) means, so that the MNs can penetrate the skin at enough depth for obtaining accurate drug delivery dose. In addition, the device of functional MNs, such as drug tip-loaded MNs, rapidly separable MNs, and gas-propelled MNs, has demonstrated a helpful means to diminish the variation in drug pharmacokinetics, as these MNs can reduce drug residue on the skin surface, resist the skin elasticity for complete MN puncture, or achieve rapid drug implantation in the skin. Another approach is to design a smart

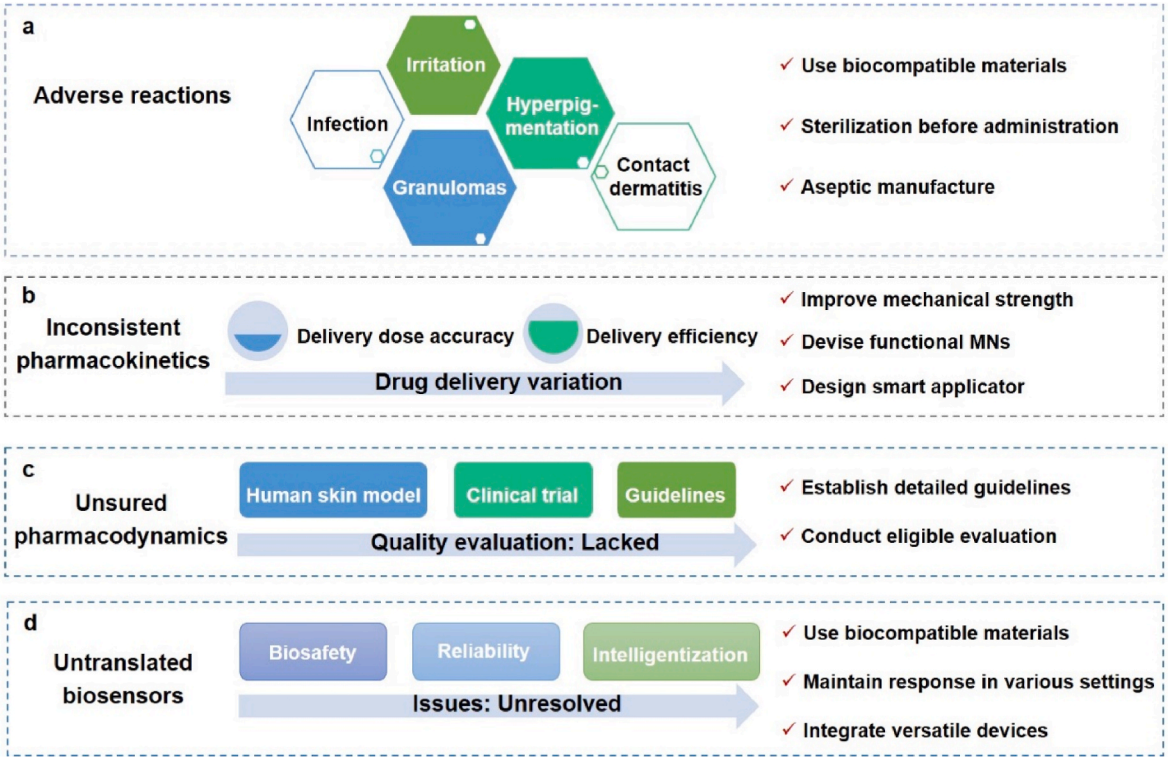

Fig. 17. Existing issues and the potential solutions involved in the clinical translation of antimicrobial MNs: (a) Various adverse reactions associated with the administration of MNs, (b) Inconsistent pharmacokinetics caused by varied drug delivery accuracy and efficiency, (c) Lack of quality evaluation guidelines to ensure pharmacodynamics, and (d) The issues of biosafety, reliability, and intelligence hinder the translation of MN-based sensors.

applicator that is capable of assisting the successful penetration of MN in the skin by adjusting the force and application time of the applicator.

Qualified microneedle product is a grantee for obtaining consistent and acceptable pharmacodynamics. However, the quality evaluation of antimicrobial MNs is still lacking of regulations and guidelines, making it challenging for the antimicrobial MNs to realize clinical translation (Fig. 17c). First, the quality evaluation criteria of MNs regarding their physicochemical properties (*e.g.*, mechanical property, skin insertion ability, drug loading capacity, transdermal delivery efficiency), have not been fully established yet, and no commercial product is available for comparison study. The lack of quality standards will bring great difficulties to the research and development of MNs. In addition, most antimicrobial MNs are currently still in the development stage, and their antimicrobial performance is mainly studied in the microbial and animal infection models. Nevertheless, the skin structures of animals are different from those of humans, and the biofilm may form a denser structure to impede the delivery of drugs in the human skin tissues, making it difficult to use animal results as an indicator of real therapeutic efficiency obtained in humans. Before the large-scale clinical application of antimicrobial MNs, there was an urgent need to conduct human skin model studies and clinical trials to disclose their real safety and pharmacodynamics. Continuous effort is also required to be paid for establishing sound regulations and guidelines to promote the antimicrobial MNs from bench to bedside.

Although there is a surge in exploring MN-based sensors as a POCT technology for personalized healthcare, the commercialization and clinical application of MN-based sensors is still confronted with the issues of biosafety, reliability, and intelligence (Fig. 17d) [176]. MN-based electrochemical sensors are one of the major types used for the detection of microbial metabolites and antibiotic concentration. However, most of the electrodes used for electrochemical biosensors consist of metallic materials (*e.g.*, platinum (Pt), Ag, Au, Ag/AgCl), which are biologically incompatible and cause potential damage to human health [177]. In addition, the large-scale manufacture of MNs with metallic electrodes is labor-intensive and highly expensive, which adds translational difficulties [178]. The 3D-printed solid MNs coated with conductive polymers have been recently proposed to address safety problems and scale up manufacture [178]. Rather than electrochemical biosensors, the integration of MNs with fluorometric systems as tattoo sensors may provide a more straightforward approach for direct target recognition [179]. The reliability of MN-based sensors remains another intractable issue, as their responses and sensitivity may vary in different conditions due to the complex interfering factors, such as physiological parameters (*e.g.*, pH and buffer strength of ISF, gender, age, disease status, skin properties), environmental factors (*e.g.*, temperature, humidity), and manual factors (*e.g.*, administration mode, operative habit) [177,180]. Moreover, the current biosensing MNs are still far from intelligence because the modules required for intelligent biosensing are usually not integrated into a single microneedle patch, such as sample collection, data processing, and information transmission [176]. It will take much effort to realize the goal of MN-mediated intelligent healthcare management.

7. Conclusion and prospects

Compared to conventional transdermal, injectable, and oral preparations, MNs offer distinct advantages in treating skin infections and hold great potential for personalized therapy in the clinic. The therapeutic efficiency of antimicrobial MNs could be improved from the following aspects: (1) Through proper optimization of the microneedle geometrics, MNs can better penetrate and adhere to the skin tissues for intradermal drug delivery. For instance, the star-like MNs were reported to have better skin penetration ability than circle, triangle, and square-like MNs, producing higher drug delivery efficiency [181]. More interestingly, the biomimetic MNs with a porcupine-like shape can form mechanical interlocking with the skin tissues and increase their adhesion to the application site [182], and those with a lamprey teeth-inspired shape can provide directional traction force to shrink

infectious wounds for auxiliary therapy [88]; (2) The introduction of external stimulus (*e.g.*, light, ultrasound, electricity, specific enzymes, nanomotors); to MNs can help the therapeutics to overcome sequential delivery barriers and produce complementary antimicrobial effects for managing intractable skin infections, including SSTI, DCFI, and biofilm-induced infections; (3) The integration of multiple antimicrobials or multifunctional nanoenzymes into MNs as an "all-in-one" therapy provides an important means to enhance antimicrobial activity and overcome antibiotic resistance; (4) The development of MN-based sensors would contribute to revolutionizing personalized anti-infection therapy, owing to their ability to identify specific pathogens, monitor disease status, and track antibiotic pharmacokinetics.

To tackle the problem of growing microbial resistance, scientists have strived to exploit innovative antimicrobials, therapeutic strategies, and detection techniques. The development of novel antimicrobials to replace antibiotics for reduced microbial resistance has become a research hotspot in recent years, such as metals [183], photosensitizers [184], sonosensitizers [185], IL [126], living bacteria [145], and NO precursors [186], owing to their unique antimicrobial mechanism. Co-delivery of multiple antimicrobial agents via MNs is another useful approach to reduce antibiotic resistance and improve antibiofilm effects by initiating synergistic antimicrobial actions. Integration of advanced biosensing technologies with MNs provides a minimally invasive approach to track the pharmacokinetics of antibiotics, which can further guide the rational and personalized dosing of antibiotics to reduce microbial resistance.

Extensive explorations have been made to promote the application of MN-based biosensors in personalized therapy. The future development of MN-based biosensors with easy-to-use and intelligent properties may be realized by these approaches: (1) The integration of detection module with MNs enables ISF extraction and biomarker analysis into one device, which will make the use of MN-based biosensors more convenient; (2) The use of advanced technologies, such as cloud storage, artificial intelligence (AI), and machine learning (ML), will help the biosensors perform data processing, computing, storage, and readout. These data provide significant information on the fluctuations in plasma drug concentration over time, which helps to guide personalized medication; (3) The connection of biosensing MNs with smartphones and medical robots will even makes it available for wireless data transmission, intelligent decision-making, and instruction execution, thus preforming medical tasks on behalf of clinicians and saving medical costs.

The wearable drug delivery with home-based therapy has becoming popular in recent years, as it provides new opportunities for treating patients who are suffering from chronic diseases and need long-term medical attention [187,188]. The MN-based wearable drug delivery usually includes delivery MNs, a MN-based biosensor, a flexible circuit board, and a wearable device. The use of advanced technology like AI and ML to manufacture wearable microneedle devices with on-demand drug delivery will come in the future. For instance, Luo et al. [189] designed a wearable closed-loop microneedle system to provide on-demand release of insulin for smart diabetes management. The wearable microneedle device consists of three parts: (1) a MN-based glucose sensor for detecting blood glucose; (2) hand piezoelectric rings and ultrasonic pumps for delivering insulin; (3) a printed circuit board (PCB) for controlling the algorithm. When the MNs penetrate the skin and contact the interstitial fluid, the sensing device is powered by PCB and the electrochemical electrode immobilized on the microneedle surface measures glucose in the interstitial fluid and further converts it into predicted blood sugar levels. Once the interstitial glucose is detected to exceed the threshold, the PCB controls the opening of the ultrasonic insulin pump through a closed-loop algorithm, and the insulin is delivered to the interstitial fluid by hollow MNs to lower blood glucose levels.

Currently, the therapeutic efficacy of antimicrobial MNs has mainly been confirmed in the microbial and animal models, and only fractional radiofrequency MNs used for treating acne vulgaris or acne scars have been subjected to clinical trials [190,191]. The paucity of clinical investigation has become a major hurdle that severely restricts the clinical translation of antimicrobial MNs. Therefore, clinical trials should be extensively conducted to establish the link between laboratory studies and clinical applications in the near future. The development of green materials and manufacturing technology is also critical for ensuring the safety and economic benefits of MNs [192].

In conclusion, antimicrobial MNs have shown broad application prospects in topical treatment and detection of skin infections. With the rapid development of tissue engineering, the application of antimicrobial MNs could also be extended to the field of wound healing and tissue regeneration. With the ongoing efforts of researchers, we believe that the current limitations involved in antimicrobial MNs will be overcome to benefit human health in the future.

CRediT authorship contribution statement

Tingting Peng: Writing – original draft, Methodology, Funding acquisition, Data curation, Conceptualization. **Yangyan Chen:** Software, Resources, Data curation. **Xuanyu Luan:** Software, Formal analysis. **Wanshan Hu:** Software, Data curation. **Wentao Wu:** Software, Data curation. **Bing Guo:** Writing – review & editing. **Chao Lu:** Writing – review & editing. **Chuanbin Wu:** Writing – review & editing, Supervision, Funding acquisition. **Xin Pan:** Writing – review & editing, Funding acquisition.

Ethics approval and consent to participate

This manuscript is a review article and no animal experiment is included in the manuscript.

Declaration of competing interest

All authors declare that there is no conflict of interest in this paper.

Acknowledgement

This work was financially supported by National Natural Science Foundation of China (82104071 and 82330112), Science Fund for Distinguished Young Scholars of Guangdong Province (2022B1515020085), Research Project of Guangdong Provincial Bureau of Traditional Chinese Medicine (20231084), and Leading Entrepreneurship Team Project of Zengcheng District (202001004).

References

[1] W. Liu, R. Gao, C. Yang, Z. Feng, W. Ou-Yang, X. Pan, P. Huang, C. Zhang, D. Kong, W. Wang, ECM-mimetic immunomodulatory hydrogel for methicillin-resistant Staphylococcus aureus-infected chronic skin wound healing, Sci. Adv. 8 (2022) eabn7006.
[2] J.S. Chin, L. Madden, S.Y. Chew, D.L. Becker, Drug therapies and delivery mechanisms to treat perturbed skin wound healing, Adv. Drug Deliv. Rev. 149–150 (2019) 2–18.
[3] Q.K. Anjani, A.H.B. Sabri, A.J. Hutton, Á. Cárcamo-Martínez, L.A.H. Wardoyo, A. Z. Mansoor, R.F. Donnelly, Microarray patches for managing infections at a global scale, J. Contr. Release 359 (2023) 97–115.
[4] V. Phatale, K.K. Vaiphei, S. Jha, D. Patil, M. Agrawal, A. Alexander, Overcoming skin barriers through advanced transdermal drug delivery approaches, J. Contr. Release 351 (2022) 361–380.
[5] L. Long, D. Ji, C. Hu, L. Yang, S. Tang, Y. Wang, Microneedles for in situ tissue regeneration, Mater Today Bio 19 (2023) 100579.
[6] H.C. Flemming, E.D. van Hullebusch, T.R. Neu, P.H. Nielsen, T. Seviour, P. Stoodley, J. Wingender, S. Wuertz, The biofilm matrix: multitasking in a shared space, Nat. Rev. Microbiol. 21 (2023) 70–86.
[7] H.-C. Flemming, J. Wingender, The biofilm matrix, Nat. Rev. Microbiol. 8 (2010) 623–633.
[8] T. Wang, E.J. Cornel, C. Li, J. Du, Drug delivery approaches for enhanced antibiofilm therapy, J. Contr. Release 353 (2023) 350–365.
[9] L.H.P. Pham, K.L. Ly, M. Colon-Ascanio, J. Ou, H. Wang, S.W. Lee, Y. Wang, J. S. Choy, K.S. Phillips, X. Luo, Dissolvable alginate hydrogel-based biofilm microreactors for antibiotic susceptibility assays, Biofilms 5 (2023) 100103.

[10] A.M. Carabelli, M. Isgró, O. Sanni, G.P. Figueredo, D.A. Winkler, L. Burroughs, A. J. Blok, J.F. Dubern, F. Pappalardo, A.L. Hook, P. Williams, M.R. Alexander, Single-cell tracking on polymer microarrays reveals the impact of surface chemistry on Pseudomonas aeruginosa twitching speed and biofilm development, ACS Appl. Bio Mater. 3 (2020) 8471–8480.
[11] L. Yang, D. Zhang, W. Li, H. Lin, C. Ding, Q. Liu, L. Wang, Z. Li, L. Mei, H. Chen, Y. Zhao, X. Zeng, Biofilm microenvironment triggered self-enhancing photodynamic immunomodulatory microneedle for diabetic wound therapy, Nat. Commun. 14 (2023) 7658.
[12] W. Zhu, J. Mei, X. Zhang, J. Zhou, D. Xu, Z. Su, S. Fang, J. Wang, X. Zhang, C. Zhu, Photothermal nanozyme-based microneedle patch against refractory bacterial biofilm infection via iron-actuated Janus ion therapy, Adv. Mater. 34 (2022) 2207961.
[13] L. Yang, Y. Yang, H. Chen, L. Mei, X. Zeng, Polymeric microneedle-mediated sustained release systems: design strategies and promising applications for drug delivery, Asian J. Pharm. Sci. 17 (2022) 70–86.
[14] Y. Zhang, Y. Xu, H. Kong, J. Zhang, H.F. Chan, J. Wang, D. Shao, Y. Tao, M. Li, Microneedle system for tissue engineering and regenerative medicine, Explorations 3 (2023) 20210170.
[15] X. Yu, J. Zhao, X. Ma, D. Fan, A multi-enzyme cascade microneedle reaction system for hierarchically MRSA biofilm elimination and diabetic wound healing, Chem. Eng. J. 465 (2023) 142933.
[16] Q. Ouyang, Y. Zeng, Y. Yu, L. Tan, X. Liu, Y. Zheng, S. Wu, Ultrasound-responsive microneedles eradicate deep-layered wound biofilm based on TiO(2) crystal phase engineering, Small 19 (2023) e2205292.
[17] L. Chen, D. Fang, J. Zhang, X. Xiao, N. Li, Y. Li, M. Wan, C. Mao, Nanomotors-loaded microneedle patches for the treatment of bacterial biofilm-related infections of wound, J. Colloid Interface Sci. 647 (2023) 142–151.
[18] W. Hu, T. Peng, Y. Huang, T. Ren, H. Chen, Y. Chen, D. Feng, C. Wu, X. Pan, Hyaluronidase-powered microneedles for significantly enhanced transdermal delivery efficiency, J. Contr. Release 353 (2023) 380–390.
[19] D.D. Zhu, L.W. Zheng, P.K. Duong, R.H. Cheah, X.Y. Liu, J.R. Wong, W.J. Wang, S. T. Tien Guan, X.T. Zheng, P. Chen, Colorimetric microneedle patches for multiplexed transdermal detection of metabolites, Biosens. Bioelectron. 212 (2022) 114412.
[20] R. Mei, Y. Wang, S. Shi, X. Zhao, Z. Zhang, X. Wang, D. Shen, Q. Kang, L. Chen, Highly sensitive and reliable internal-standard surface-enhanced Raman scattering microneedles for determination of bacterial metabolites as infection biomarkers in skin interstitial fluid, Anal. Chem. 94 (2022) 16069–16078.
[21] F. Tehrani, H. Teymourian, B. Wuerstle, J. Kavner, R. Patel, A. Furmidge, R. Aghavali, H. Hosseini-Toudeshki, C. Brown, F. Zhang, K. Mahato, Z. Li, A. Barfidokht, L. Yin, P. Warren, N. Huang, Z. Patel, P.P. Mercier, J. Wang, An integrated wearable microneedle array for the continuous monitoring of multiple biomarkers in interstitial fluid, Nat. Biomed. Eng. 6 (2022) 1214–1224.
[22] H. Sun, Y. Zheng, G. Shi, H. Haick, M. Zhang, Wearable clinic: from microneedle-based sensors to next-generation healthcare platforms, Small (2023) e2207539.
[23] S. Lin, X. Cheng, J. Zhu, B. Wang, D. Jelinek, Y. Zhao, T.Y. Wu, A. Horrillo, J. Tan, J. Yeung, W. Yan, S. Forman, H.A. Coller, C. Milla, S. Emaminejad, Wearable microneedle-based electrochemical aptamer biosensing for precision dosing of drugs with narrow therapeutic windows, Sci. Adv. 8 (2022) eabq4539.
[24] T.M. Rawson, S.A.N. Gowers, D.M.E. Freeman, R.C. Wilson, S. Sharma, M. Gilchrist, A. MacGowan, A. Lovering, M. Bayliss, M. Kyriakides, P. Georgiou, A.E.G. Cass, D. O'Hare, A.H. Holmes, Microneedle biosensors for real-time, minimally invasive drug monitoring of phenoxymethylpenicillin: a first-in-human evaluation in healthy volunteers, Lancet Digit Health 1 (2019) e335–e343.
[25] P.P. Samant, M.M. Niedzwiecki, N. Raviele, V. Tran, J. Mena-Lapaix, D.I. Walker, E.I. Felner, D.P. Jones, G.W. Miller, M.R. Prausnitz, Sampling interstitial fluid from human skin using a microneedle patch, Sci. Transl. Med. 12 (2020).
[26] Y. Xiang, J. Lu, C. Mao, Y. Zhu, C. Wang, J. Wu, X. Liu, S. Wu, K.Y.H. Kwan, K.M. C. Cheung, K.W.K. Yeung, Ultrasound-triggered interfacial engineering-based microneedle for bacterial infection acne treatment, Sci. Adv. 9 (2023) eadf0854.
[27] S. Li, X. Wang, Z. Yan, T. Wang, Z. Chen, H. Song, Y. Zheng, Microneedle patches with antimicrobial and immunomodulating properties for infected wound healing, Adv. Sci. 10 (2023) e2300576.
[28] M. Rezapour Sarabi, S.A. Nakhjavani, S. Tasoglu, 3D-printed microneedles for point-of-care biosensing applications, Micromachines 13 (2022).
[29] A.S. Moffarah, M. Al Mohajer, B.L. Hurwitz, D.G. Armstrong, Skin and soft tissue infections, Microbiol. Spectr. 4 (2016).
[30] C. Walsh, Where will new antibiotics come from? Nat. Rev. Microbiol. 1 (2003) 65–70.
[31] R.P. Cook, M.B. Brown, Effect of the source of nitrogen in the medium on the formation of penicillin by surface cultures of Penicillium notatum, Nature 159 (1947) 376.
[32] J. Clardy, M.A. Fischbach, C.R. Currie, The natural history of antibiotics, Curr. Biol. 19 (2009) R437–R441.
[33] J.S. Puls, D. Brajtenbach, T. Schneider, U. Kubitscheck, F. Grein, Inhibition of peptidoglycan synthesis is sufficient for total arrest of staphylococcal cell division, Sci. Adv. 9 (2023) eade9023.
[34] J.G. Hurdle, A.J. O'Neill, I. Chopra, R.E. Lee, Targeting bacterial membrane function: an underexploited mechanism for treating persistent infections, Nat. Rev. Microbiol. 9 (2011) 62–75.
[35] D.N. Wilson, Ribosome-targeting antibiotics and mechanisms of bacterial resistance, Nat. Rev. Microbiol. 12 (2014) 35–48.
[36] Q. Jin, X. Xie, Y. Zhai, H. Zhang, Mechanisms of folate metabolism-related substances affecting Staphylococcus aureus infection, Int J Med Microbiol 313 (2023) 151577.
[37] J. Xu, R. Danehy, H. Cai, Z. Ao, M. Pu, A. Nusawardhana, D. Rowe-Magnus, F. Guo, Microneedle patch-mediated treatment of bacterial biofilms, ACS Appl. Mater. Interfaces 11 (2019) 14640–14646.
[38] S.D. Gittard, A. Ovsianikov, H. Akar, B. Chichkov, N.A. Monteiro-Riviere, S. Stafslien, B. Chisholm, C.C. Shin, C.M. Shih, S.J. Lin, Y.Y. Su, R.J. Narayan, Two photon polymerization-micromolding of polyethylene glycol-gentamicin sulfate microneedles, Adv. Eng. Mater. 12 (2010) B77–b82.
[39] F. Keyvani, P. GhavamiNejad, M.A. Saleh, M. Soltani, Y. Zhao, S. Sadeghzadeh, A. Shakeri, P. Chelle, H. Zheng, F.A. Rahman, S. Mahshid, J. Quadrilatero, P.P. N. Rao, A. Edginton, M. Poudineh, Integrated electrochemical aptamer biosensing and colorimetric pH monitoring via hydrogel microneedle assays for assessing antibiotic treatment, Adv. Sci. 9 (2024) e2309027.
[40] M. Mir, A.D. Permana, I.A. Tekko, H.O. McCarthy, N. Ahmed, A.U. Rehman, R. F. Donnelly, Microneedle liquid injection system assisted delivery of infection responsive nanoparticles: a promising approach for enhanced site-specific delivery of carvacrol against polymicrobial biofilms-infected wounds, Int. J. Pharm. 587 (2020) 119643.
[41] J. Ziesmer, P. Tajpara, N.J. Hempel, M. Ehrström, K. Melican, L. Eidsmo, G. A. Sotiriou, Vancomycin-loaded microneedle arrays against methicillin-resistant Staphylococcus aureus skin infections, Adv Mater Technol 6 (2021) 2001307.
[42] M.S. Arshad, A.T. Zahra, S. Zafar, H. Zaman, A. Akhtar, M.M. Ayaz, I. Kucuk, M. Maniruzzaman, M.W. Chang, Z. Ahmad, Antibiofilm effects of macrolide loaded microneedle patches: prospects in healing infected wounds, Pharm. Res. (N. Y.) 38 (2021) 165–177.
[43] Y. Zhang, P. Feng, J. Yu, J. Yang, J. Zhao, J. Wang, Q. Shen, Z. Gu, ROS-responsive microneedle patch for acne vulgaris treatment, Adv. Ther. 1 (2018) 1800035.
[44] J.G. Turner, M. Laabei, S. Li, P. Estrela, H.S. Leese, Antimicrobial releasing hydrogel forming microneedles, Biomater. Adv. 151 (2023) 213467.
[45] M. Mudjahid, F. Nainu, R.N. Utami, A. Sam, A.N.F. Marzaman, T.P. Roska, R. M. Asri, A. Himawan, R.F. Donnelly, A.D. Permana, Enhancement in site-specific delivery of chloramphenicol using bacterially densitive microparticle loaded into dissolving microneedle: potential for enhanced effectiveness treatment of cellulitis, ACS Appl. Mater. Interfaces 14 (2022) 56560–56577.
[46] S. Zafar, M.S. Arshad, S.J. Rana, M. Patel, B. Yousef, Z. Ahmad, Engineering of clarithromycin loaded stimulus responsive dissolving microneedle patches for the treatment of biofilms, Int. J. Pharm. 640 (2023) 123003.
[47] F. Pinheiro da Silva, M.C. Machado, Antimicrobial peptides: clinical relevance and therapeutic implications, Peptides 36 (2012) 308–314.
[48] L.-j. Zhang, R.L. Gallo, Antimicrobial peptides, Curr. Biol. 26 (2016) R14–R19.
[49] L. Lin, J. Chi, Y. Yan, R. Luo, X. Feng, Y. Zheng, D. Xian, X. Li, G. Quan, D. Liu, C. Wu, C. Lu, X. Pan, Membrane-disruptive peptides/peptidomimetics-based therapeutics: promising systems to combat bacteria and cancer in the drug-resistant era, Acta Pharm. Sin. B 11 (2021) 2609–2644.
[50] M. Magana, M. Pushpanathan, A.L. Santos, L. Leanse, M. Fernandez, A. Ioannidis, M.A. Giulianotti, Y. Apidianakis, S. Bradfute, A.L. Ferguson, A. Cherkasov, M. N. Seleem, C. Pinilla, C. de la Fuente-Nunez, T. Lazaridis, T. Dai, R.A. Houghten, R.E.W. Hancock, G.P. Tegos, The value of antimicrobial peptides in the age of resistance, Lancet Infect. Dis. 20 (2020) e216–e230.
[51] Y. Su, V.L. Mainardi, H. Wang, A. McCarthy, Y.S. Zhang, S. Chen, J.V. John, S. L. Wong, R.R. Hollins, G. Wang, J. Xie, Dissolvable microneedles coupled with nanofiber dressings eradicate biofilms via effectively delivering a database-designed antimicrobial peptide, ACS Nano 14 (2020) 11775–11786.
[52] A. Hossain, M.A. Ali, L. Lin, J. Luo, Y. You, M.M.I. Masum, Y. Jiang, Y. Wang, B. Li, Q. An, Biocontrol of soft rot dickeya and pectobacterium pathogens by broad-spectrum antagonistic bacteria within Paenibacillus polymyxa complex, Microorganisms 11 (2023) 817.
[53] S.A. Yuk, H. Kim, N.S. Abutaleb, A.M. Dieterly, M.S. Taha, M.D. Tsifansky, L. T. Lyle, M.N. Seleem, Y. Yeo, Nanocapsules modify membrane interaction of polymyxin B to enable safe systemic therapy of Gram-negative sepsis, Sci. Adv. 7 (2021) eabj1577.
[54] X. Lai, M.L. Han, Y. Ding, S.H. Chow, A.P. Le Brun, C.M. Wu, P.J. Bergen, J. H. Jiang, H.Y. Hsu, B.W. Muir, J. White, J. Song, J. Li, H.H. Shen, A polytherapy based approach to combat antimicrobial resistance using cubosomes, Nat. Commun. 13 (2022) 343.
[55] X. Zhang, G. Chen, Y. Yu, L. Sun, Y. Zhao, Bioinspired adhesive and antibacterial microneedles for versatile transdermal drug delivery, Research (2020) 3672120.
[56] Z. Badran, B. Rahman, P. De Bonfils, P. Nun, V. Coeffard, E. Verron, Antibacterial nanophotosensitizers in photodynamic therapy: an update, Drug Discov. Today 28 (2023) 103493.
[57] X. Pang, D. Li, J. Zhu, J. Cheng, G. Liu, Beyond antibiotics: photo/sonodynamic approaches for bacterial theranostics, Nano-Micro Lett. 12 (2020) 144.
[58] F. Cieplik, D. Deng, W. Crielaard, W. Buchalla, E. Hellwig, A. Al-Ahmad, T. Maisch, Antimicrobial photodynamic therapy - what we know and what we don't, Crit. Rev. Microbiol. 44 (2018) 571–589.
[59] C.S. Foote, Definition of type I and type II photosensitized oxidation, Photochem. Photobiol. 54 (1991) 659.
[60] M. Wainwright, Photodynamic antimicrobial chemotherapy (PACT), J. Antimicrob. Chemother. 42 (1998) 13–28.
[61] T. Wen, Z. Lin, Y. Zhao, Y. Zhou, B. Niu, C. Shi, C. Lu, X. Wen, M. Zhang, G. Quan, C. Wu, X. Pan, Bioresponsive nanoarchitectonics-integrated microneedles for amplified chemo-photodynamic therapy against acne vulgaris, ACS Appl. Mater. Interfaces 13 (2021) 48433–48448.
[62] E. Caffarel-Salvador, M.-C. Kearney, R. Mairs, L. Gallo, S.A. Stewart, A.J. Brady, R.F. Donnelly, Methylene blue-loaded dissolving microneedles: potential use in

photodynamic antimicrobial chemotherapy of infected wounds, Pharmaceutics 7 (2015) 397–412.
[63] H. Wang, Y. Fu, S. Du, P. Liu, J. Ren, Y. Liu, J. Tao, L. Zhang, J. Zhu, Mechanically robust dissolving microneedles made of supramolecular photosensitizers for effective photodynamic bacterial biofilm elimination, ACS Appl. Mater. Interfaces 15 (2023) 25417–25426.
[64] J.H. Gong, L.J. Chen, X. Zhao, X.P. Yan, Persistent production of reactive oxygen species with Zn(2)GeO(4):Cu Nanorod-loaded microneedles for methicillin-resistant Staphylococcus aureus infectious wound healing, ACS Appl. Mater. Interfaces 14 (2022) 17142–17152.
[65] X.-L. Lei, K. Cheng, Y. Li, Z.-T. Zhong, X.-L. Hou, L.-B. Song, F. Zhang, J.-H. Wang, Y.-D. Zhao, Q.-R. Xu, The eradication of biofilm for therapy of bacterial infected chronic wound based on pH-responsive micelle of antimicrobial peptide derived biodegradable microneedle patch, Chem. Eng. J. 462 (2023) 142222.
[66] J. Huo, Q. Jia, H. Huang, J. Zhang, P. Li, X. Dong, W. Huang, Emerging photothermal-derived multimodal synergistic therapy in combating bacterial infections, Chem. Soc. Rev. 50 (2021) 8762–8789.
[67] L. Chen, M. Peng, J. Zhou, X. Hu, Y. Piao, H. Li, R. Hu, Y. Li, L. Shi, Y. Liu, Supramolecular photothermal cascade nano-reactor enables photothermal effect, cascade reaction, and in situ hydrogelation for biofilm-associated tooth-extraction wound healing, Adv. Mater. 35 (2023) e2301664.
[68] Y. Jiang, J. Huang, C. Xu, K. Pu, Activatable polymer nanoagonist for second near-infrared photothermal immunotherapy of cancer, Nat. Commun. 12 (2021) 742.
[69] Y. Chen, Y. Gao, Y. Chen, L. Liu, A. Mo, Q. Peng, Nanomaterials-based photothermal therapy and its potentials in antibacterial treatment, J. Contr. Release 328 (2020) 251–262.
[70] X. Wu, Y. Suo, H. Shi, R. Liu, F. Wu, T. Wang, L. Ma, H. Liu, Z. Cheng, Deep-tissue photothermal therapy using laser illumination at NIR-IIa window, Nano-Micro Lett. 12 (2020) 38.
[71] G. Hong, S. Diao, J. Chang, A.L. Antaris, C. Chen, B. Zhang, S. Zhao, D.N. Atochin, P.L. Huang, K.I. Andreasson, C.J. Kuo, H. Dai, Through-skull fluorescence imaging of the brain in a new near-infrared window, Nat. Photonics 8 (2014) 723–730.
[72] X. Lei, M. Li, C. Wang, P. Cui, L. Qiu, S. Zhou, P. Jiang, H. Li, D. Zhao, X. Ni, J. Wang, J. Xia, Degradable microneedle patches loaded with antibacterial gelatin nanoparticles to treat staphylococcal infection-induced chronic wounds, Int. J. Biol. Macromol. 217 (2022) 55–65.
[73] Y. Chen, Y. Gao, Y. Chen, L. Liu, A. Mo, Q. Peng, Nanomaterials-based photothermal therapy and its potentials in antibacterial treatment, J. Contr. Release 328 (2020) 251–262.
[74] P. Zhao, Y. Zhang, X. Chen, C. Xu, J. Guo, M. Deng, X. Qu, P. Huang, Z. Feng, J. Zhang, Versatile hydrogel dressing with skin adaptiveness and mild photothermal antibacterial activity for methicillin-resistant Staphylococcus aureus-infected dynamic wound healing, Adv. Sci. 10 (2023) e2206585.
[75] X. Feng, D. Xian, J. Fu, R. Luo, W. Wang, Y. Zheng, Q. He, Z. Ouyang, S. Fang, W. Zhang, D. Liu, S. Tang, G. Quan, J. Cai, C. Wu, C. Lu, X. Pan, Four-armed host-defense peptidomimetics-augmented vanadium carbide MXene-based microneedle array for efficient photo-excited bacteria-killing, Chem. Eng. J. 456 (2023) 141121.
[76] X. Yu, J. Zhao, D. Fan, A dissolving microneedle patch for Antibiotic/Enzymolysis/Photothermal triple therapy against bacteria and their biofilms, Chem. Eng. J. (Lausanne) 437 (2022) 135475.
[77] Y. Su, S.M. Andrabi, S.M.S. Shahriar, S.L. Wong, G. Wang, J. Xie, Triggered release of antimicrobial peptide from microneedle patches for treatment of wound biofilms, J. Contr. Release 356 (2023) 131–141.
[78] J.L. Hobman, L.C. Crossman, Bacterial antimicrobial metal ion resistance, J. Med. Microbiol. 64 (2015) 471–497.
[79] S. Chernousova, M. Epple, Silver as antibacterial agent: ion, nanoparticle, and metal, Angew Chem. Int. Ed. Engl. 52 (2013) 1636–1653.
[80] S. Tang, J. Zheng, Antibacterial activity of silver nanoparticles: structural effects, Adv. Healthcare Mater. 7 (2018) e1701503.
[81] Y. Liu, Y. Lu, Z. Xu, X. Ma, X. Chen, W. Liu, Repurposing of the gold drug auranofin and a review of its derivatives as antibacterial therapeutics, Drug Discov. Today 27 (2022) 1961–1973.
[82] S. Li, S. Dong, W. Xu, S. Tu, L. Yan, C. Zhao, J. Ding, X. Chen, Antibacterial hydrogels, Adv. Sci. 5 (2018) 1700527.
[83] X. Yi, J. He, X. Wang, Y. Zhang, G. Tan, Z. Zhou, J. Chen, D. Chen, R. Wang, W. Tian, P. Yu, L. Zhou, C. Ning, Tunable mechanical, antibacterial, and cytocompatible hydrogels based on a functionalized dual network of metal coordination bonds and covalent crosslinking, ACS Appl. Mater. Interfaces 10 (2018) 6190–6198.
[84] S.D. Gittard, P.R. Miller, C. Jin, T.N. Martin, R.D. Boehm, B.J. Chisholm, S. J. Stafslien, J.W. Daniels, N. Cilz, N.A. Monteiro-Riviere, A. Nasir, R.J. Narayan, Deposition of antimicrobial coatings on microstereolithography-fabricated microneedles, J. Miner. Met. Mater. Soc. 63 (2011) 59–68.
[85] S. Yao, J. Chi, Y. Wang, Y. Zhao, Y. Luo, Y. Wang, Zn-MOF encapsulated antibacterial and degradable microneedles array for promoting wound healing, Adv. Healthcare Mater. 10 (2021) 2100056.
[86] C. Gunawan, C.P. Marquis, R. Amal, G.A. Sotiriou, S.A. Rice, E.J. Harry, Widespread and indiscriminate nanosilver use: genuine potential for microbial resistance, ACS Nano 11 (2017) 3438–3445.
[87] L.E. González García, M.N. MacGregor, R.M. Visalakshan, N. Ninan, A. A. Cavallaro, A.D. Trinidad, Y. Zhao, A.J.D. Hayball, K. Vasilev, Self-sterilizing antibacterial silver-loaded microneedles, Chem. Commun. 55 (2018) 171–174.
[88] Y. Deng, C. Yang, Y. Zhu, W. Liu, H. Li, L. Wang, W. Chen, Z. Wang, L. Wang, Lamprey-teeth-inspired oriented antibacterial sericin microneedles for infected wound healing improvement, Nano Lett. 22 (2022) 2702–2711.
[89] Z. Lu, S. Du, J. Li, M. Zhang, H. Nie, X. Zhou, F. Li, X. Wei, J. Wang, F. Liu, C. He, G. Yang, Z. Gu, Langmuir-Blodgett-mediated formation of antibacterial microneedles for long-term transdermal drug delivery, Adv. Mater. 35 (2023) e2303388.
[90] C. Zhang, W. Bu, D. Ni, S. Zhang, Q. Li, Z. Yao, J. Zhang, H. Yao, Z. Wang, J. Shi, Synthesis of iron nanometallic glasses and their application in cancer therapy by a localized Fenton reaction, Angew Chem. Int. Ed. Engl. 55 (2016) 2101–2106.
[91] Y. Xu, L. Xiao, J. Chen, Q. Wu, W. Yu, W. Zeng, Y. Shi, Y. Lu, Y. Liu, α-Fe(2)O(3) based nanotherapeutics for near-infrared/dihydroartemisinin dual-augmented chemodynamic antibacterial therapy, Acta Biomater. 150 (2022) 367–379.
[92] C. Jia, Y. Guo, F.-G. Wu, Chemodynamic therapy via Fenton and Fenton-like nanomaterials: strategies and recent advances, Small 18 (2022) 2103868.
[93] M. Kharaziha, A. Baidya, N. Annabi, Rational design of immunomodulatory hydrogels for chronic wound healing, Adv. Mater. 33 (2021) e2100176.
[94] Y. Zhang, X. Zhang, H. Yang, L. Yu, Y. Xu, A. Sharma, P. Yin, X. Li, J.S. Kim, Y. Sun, Advanced biotechnology-assisted precise sonodynamic therapy, Chem. Soc. Rev. 50 (2021) 11227–11248.
[95] R. Canaparo, F. Foglietta, N. Barbero, L. Serpe, The promising interplay between sonodynamic therapy and nanomedicine, Adv. Drug Deliv. Rev. 189 (2022) 114495.
[96] R. Wang, Q. Liu, A. Gao, N. Tang, Q. Zhang, A. Zhang, D. Cui, Recent developments of sonodynamic therapy in antibacterial application, Nanoscale 14 (2022) 12999–13017.
[97] H. Lea-Banks, M.A. O'Reilly, K. Hynynen, Ultrasound-responsive droplets for therapy: a review, J. Contr. Release 293 (2019) 144–154.
[98] X. Qian, Y. Zheng, Y. Chen, Micro/nanoparticle-augmented sonodynamic therapy (SDT): breaking the depth shallow of photoactivation, Adv. Mater. 28 (2016) 8097–8129.
[99] X. Li, S. Lee, J. Yoon, Supramolecular photosensitizers rejuvenate photodynamic therapy, Chem. Soc. Rev. 47 (2018) 1174–1188.
[100] W. Guan, L. Tan, X. Liu, Z. Cui, Y. Zheng, K.W.K. Yeung, D. Zheng, Y. Liang, Z. Li, S. Zhu, X. Wang, S. Wu, Ultrasonic interfacial engineering of red phosphorous-metal for eradicating MRSA infection effectively, Adv. Mater. 33 (2021) e2006047.
[101] X. He, J.-T. Hou, X. Sun, P. Jangili, J. An, Y. Qian, J.S. Kim, J. Shen, NIR-II photo-amplified sonodynamic therapy using sodium molybdenum bronze nanoplatform against subcutaneous Staphylococcus aureus infection, Adv. Funct. Mater. 32 (2022) 2203964.
[102] X. Wang, X. Zhong, L. Bai, J. Xu, F. Gong, Z. Dong, Z. Yang, Z. Zeng, Z. Liu, L. Cheng, Ultrafine titanium monoxide (TiO(1+x)) nanorods for enhanced sonodynamic therapy, J. Am. Chem. Soc. 142 (2020) 6527–6537.
[103] Q. Ouyang, Y. Zeng, Y. Yu, L. Tan, X. Liu, Y. Zheng, S. Wu, Ultrasound-responsive microneedles eradicate deep-layered wound biofilm based on TiO_2 crystal phase engineering, Small 19 (2023) 2205292.
[104] M. Liang, L. Shang, Y. Yu, Y. Jiang, Q. Bai, J. Ma, D. Yang, N. Sui, Z. Zhu, Ultrasound activatable microneedles for bilaterally augmented sono-chemodynamic and sonothermal antibacterial therapy, Acta Biomater. 158 (2023) 811–826.
[105] C. Cox, Elizabeth Evans Hughes–surviving starvation therapy for diabetes, Lancet 377 (2011) 1232–1233.
[106] J. Folkman, Tumor angiogenesis: therapeutic implications, N. Engl. J. Med. 285 (1971) 1182–1186.
[107] L. Peng, X. Yang, S. Wang, Y.K. Chan, Y. Chen, Z. Yang, Y. Mao, L. Li, W. Yang, Y. Deng, Bimetal metal-organic framework domino micro-reactor for synergistic antibacterial starvation/chemodynamic therapy and robust wound healing, Nanoscale 14 (2022) 2052–2064.
[108] D. Li, T. Chen, Y. Zhang, Y. Xu, H. Niu, Synergistical starvation and chemo-dynamic therapy for combating multidrug-resistant bacteria and accelerating diabetic wound healing, Adv. Healthcare Mater. 10 (2021) 2100716.
[109] M. Zhao, M. Zhou, P. Gao, X. Zheng, W. Yu, Z. Wang, J. Li, J. Zhang, AgNPs/nGOx/Apra nanocomposites for synergistic antimicrobial therapy and scarless skin recovery, J. Mater. Chem. B 10 (2022) 1393–1402.
[110] J. Shan, X. Zhang, Y. Cheng, C. Song, G. Chen, Z. Gu, Y. Zhao, Glucose metabolism-inspired catalytic patches for NIR-II phototherapy of diabetic wound infection, Acta Biomater. 157 (2023) 200–209.
[111] F. Manea, F.B. Houillon, L. Pasquato, P. Scrimin, Nanozymes: gold-nanoparticle-based transphosphorylation catalysts, Angew Chem. Int. Ed. Engl. 43 (2004) 6165–6169.
[112] L. Gao, J. Zhuang, L. Nie, J. Zhang, Y. Zhang, N. Gu, T. Wang, J. Feng, D. Yang, S. Perrett, X. Yan, Intrinsic peroxidase-like activity of ferromagnetic nanoparticles, Nat. Nanotechnol. 2 (2007) 577–583.
[113] H. Wei, E. Wang, Nanomaterials with enzyme-like characteristics (nanozymes): next-generation artificial enzymes, Chem. Soc. Rev. 42 (2013) 6060–6093.
[114] F. Cheng, S. Wang, H. Zheng, H. Shen, L. Zhou, Z. Yang, Q. Li, Q. Zhang, H. Zhang, Ceria nanoenzyme-based hydrogel with antiglycative and antioxidative performance for infected diabetic wound healing, Small Methods 6 (2022) 2200949.
[115] S. Wang, H. Zheng, L. Zhou, F. Cheng, Z. Liu, H. Zhang, L. Wang, Q. Zhang, Nanoenzyme-reinforced injectable hydrogel for healing diabetic wounds infected with multidrug resistant bacteria, Nano Lett. 20 (2020) 5149–5158.
[116] Y. Tao, E. Ju, J. Ren, X. Qu, Bifunctionalized mesoporous silica-supported gold nanoparticles: intrinsic oxidase and peroxidase catalytic activities for antibacterial applications, Adv. Mater. 27 (2015) 1097–1104.

[117] J. Wang, Y. Wang, D. Zhang, C. Chen, Intrinsic oxidase-like nanoenzyme Co_4S_3/$Co(OH)_2$ hybrid nanotubes with broad-spectrum antibacterial activity, ACS Appl. Mater. Interfaces 12 (2020) 29614–29624.
[118] J. Shi, R. Shu, X. Shi, Y. Li, J. Li, Y. Deng, W. Yang, Multi-activity cobalt ferrite/MXene nanoenzymes for drug-free phototherapy in bacterial infection treatment, RSC Adv. 12 (2022) 11090–11099.
[119] D. Sun, X. Pang, Y. Cheng, J. Ming, S. Xiang, C. Zhang, P. Lv, C. Chu, X. Chen, G. Liu, N. Zheng, Ultrasound-switchable nanozyme augments sonodynamic therapy against multidrug-resistant bacterial infection, ACS Nano 14 (2020) 2063–2076.
[120] K. Huang, W. Liu, W. Wei, Y. Zhao, P. Zhuang, X. Wang, Y. Wang, Y. Hu, H. Dai, Photothermal hydrogel encapsulating intelligently bacteria-capturing bio-MOF for infectious wound healing, ACS Nano 16 (2022) 19491–19508.
[121] J. Shan, X. Zhang, L. Wang, Y. Zhao, Spatiotemporal catalytic nanozymes microneedle patches with opposite properties for wound management, Small 19 (2023) e2302347.
[122] W.H. Chen, M. Vázquez-González, A. Kozell, A. Cecconello, I. Willner, Cu^{2+}-modified metal-organic framework nanoparticles: a peroxidase-mimicking nanoenzyme, Small 14 (2018).
[123] Z. Yan, W. Bing, C. Ding, K. Dong, J. Ren, X. Qu, A H_2O_2-free depot for treating bacterial infection: localized cascade reactions to eradicate biofilms in vivo, Nanoscale 10 (2018) 17656–17662.
[124] N. Singh, G.R. Sherin, G. Mugesh, Antioxidant and prooxidant nanozymes: from cellular redox regulation to next-generation therapeutics, Angew Chem. Int. Ed. Engl. 62 (2023) e202301232.
[125] S. Shi, Y. Jiang, Y. Yu, M. Liang, Q. Bai, L. Wang, D. Yang, N. Sui, Z. Zhu, Piezo-augmented and photocatalytic nanozyme integrated microneedles for antibacterial and anti-inflammatory combination therapy, Adv. Funct. Mater. 33 (2023) 2210850.
[126] L. Zheng, J. Li, M. Yu, W. Jia, S. Duan, D. Cao, X. Ding, B. Yu, X. Zhang, F.J. Xu, Molecular sizes and antibacterial performance relationships of flexible ionic liquid derivatives, J. Am. Chem. Soc. 142 (2020) 20257–20269.
[127] J. Shi, M. Wang, Z. Sun, Y. Liu, J. Guo, H. Mao, F. Yan, Aggregation-induced emission-based ionic liquids for bacterial killing, imaging, cell labeling, and bacterial detection in blood cells, Acta Biomater. 97 (2019) 247–259.
[128] J. Qin, J. Guo, Q. Xu, Z. Zheng, H. Mao, F. Yan, Synthesis of pyrrolidinium-type poly(ionic liquid) membranes for antibacterial applications, ACS Appl. Mater. Interfaces 9 (2017) 10504–10511.
[129] T. Zhang, B. Sun, J. Guo, M. Wang, H. Cui, H. Mao, B. Wang, F. Yan, Active pharmaceutical ingredient poly(ionic liquid)-based microneedles for the treatment of skin acne infection, Acta Biomater. 115 (2020) 136–147.
[130] X. Chao, C. Zhang, X. Li, H. Lv, G. Ling, P. Zhang, Synthesis and characterization of ionic liquid microneedle patches with different carbon chain lengths for antibacterial application, Biomater. Sci. 10 (2022) 1008–1017.
[131] Y. Li, X. Hu, Z. Dong, Y. Chen, W. Zhao, Y. Wang, L. Zhang, M. Chen, C. Wu, Q. Wang, Dissolving microneedle arrays with optimized needle geometry for transcutaneous immunization, Eur. J. Pharmaceut. Sci. 151 (2020) 105361.
[132] Y. Huang, T. Peng, W. Hu, X. Gao, Y. Chen, Q. Zhang, C. Wu, X. Pan, Fully armed photodynamic therapy with spear and shear for topical deep hypertrophic scar treatment, J. Contr. Release 343 (2022) 408–419.
[133] B.E. Shields, M. Rosenbach, Z. Brown-Joel, A.P. Berger, B.A. Ford, K.A. Wanat, Angioinvasive fungal infections impacting the skin: background, epidemiology, and clinical presentation, J. Am. Acad. Dermatol. 80 (2019) 869–880.e865.
[134] J.E. Carpouron, S. de Hoog, E. Gentekaki, K.D. Hyde, Emerging animal-associated fungal diseases, J Fungi 8 (2022) 611.
[135] S.D. Gunaydin, S. Arikan-Akdagli, M. Akova, Fungal infections of the skin and soft tissue, Curr. Opin. Infect. Dis. 33 (2020) 130–136.
[136] R.D. Boehm, P.R. Miller, W.A. Schell, J.R. Perfect, R.J. Narayan, Inkjet printing of Amphotericin B onto biodegradable microneedles using piezoelectric inkjet printing, J. Miner. Met. Mater. Soc. 65 (2013) 525–533.
[137] R.F. Donnelly, E. Larrañeta, Microarray patches: potentially useful delivery systems for long-acting nanosuspensions, Drug Discov. Today 23 (2018) 1026–1033.
[138] M.I. Nasiri, L.K. Vora, J.A. Ershaid, K. Peng, I.A. Tekko, R.F. Donnelly, Nanoemulsion-based dissolving microneedle arrays for enhanced intradermal and transdermal delivery, Drug Deliv Transl Res 12 (2022) 881–896.
[139] A.D. Permana, A.J. Paredes, F. Volpe-Zanutto, Q.K. Anjani, E. Utomo, R. F. Donnelly, Dissolving microneedle-mediated dermal delivery of itraconazole nanocrystals for improved treatment of cutaneous candidiasis, Eur. J. Pharm. Biopharm. 154 (2020) 50–61.
[140] K. Peng, L.K. Vora, J. Domínguez-Robles, Y.A. Naser, M. Li, E. Larrañeta, R. F. Donnelly, Hydrogel-forming microneedles for rapid and efficient skin deposition of controlled release tip-implants, Mater. Sci. Eng., C 127 (2021) 112226.
[141] B. Wang, W. Zhang, Q. Pan, J. Tao, S. Li, T. Jiang, X. Zhao, Hyaluronic acid-based CuS nanoenzyme biodegradable microneedles for treating feep cutaneous fungal infection without drug resistance, Nano Lett. 23 (2023) 1327–1336.
[142] M. Raffatellu, Learning from bacterial competition in the host to develop antimicrobials, Nat. Med. 24 (2018) 1097–1103.
[143] Y. Flores Bueso, P. Lehouritis, M. Tangney, In situ biomolecule production by bacteria; a synthetic biology approach to medicine, J. Contr. Release 275 (2018) 217–228.
[144] P. Piewngam, Y. Zheng, T.H. Nguyen, S.W. Dickey, H.S. Joo, A.E. Villaruz, K. A. Glose, E.L. Fisher, R.L. Hunt, B. Li, J. Chiou, S. Pharkjaksu, S. Khongthong, G.Y. C. Cheung, P. Kiratisin, M. Otto, Pathogen elimination by probiotic Bacillus via signalling interference, Nature 562 (2018) 532–537.
[145] F. Wang, X. Zhang, G. Chen, Y. Zhao, Living bacterial microneedles for fungal infection treatment, Research 2020 (2020) 2760594.
[146] Z. Wang, A. Jin, Z. Yang, W. Huang, Advanced nitric oxide generating nanomedicine for therapeutic applications, ACS Nano 17 (2023) 8935–8965.
[147] X. Bao, S. Zheng, L. Zhang, A. Shen, G. Zhang, S. Liu, J. Hu, Nitric-oxide-releasing aza-BODIPY: a new near-infrared J-aggregate with multiple antibacterial modalities, Angew Chem. Int. Ed. Engl. 61 (2022) e202207250.
[148] D. Hu, Y. Deng, F. Jia, Q. Jin, J. Ji, Surface charge switchable supramolecular nanocarriers for nitric oxide synergistic photodynamic eradication of biofilms, ACS Nano 14 (2020) 347–359.
[149] M. Garren, P. Maffe, A. Melvin, L. Griffin, S. Wilson, M. Douglass, M. Reynolds, H. Handa, Surface-catalyzed nitric oxide release via a metal organic framework enhances antibacterial surface effects, ACS Appl. Mater. Interfaces 13 (2021) 56931–56943.
[150] E. Chugunova, N. Akylbekov, A. Bulatova, N. Gavrilov, A. Voloshina, N. Kulik, V. Zobov, A. Dobrynin, V. Syakaev, A. Burilov, Synthesis and biological evaluation of novel structural hybrids of benzofuroxan derivatives and fluoroquinolones, Eur. J. Med. Chem. 116 (2016) 165–172.
[151] S. Liu, X. Cai, W. Xue, D. Ma, W. Zhang, Chitosan derivatives co-delivering nitric oxide and methicillin for the effective therapy to the methicillin-resistant S. aureus infection, Carbohydr. Polym. 234 (2020) 115928.
[152] Q. Zhang, Z. Zhang, X. Zou, Z. Liu, Q. Li, J. Zhou, S. Gao, H. Xu, J. Guo, F. Yan, Nitric oxide-releasing poly(ionic liquid)-based microneedle for subcutaneous fungal infection treatment, Biomater. Sci. 11 (2023) 3114–3127.
[153] U. Nagra, K. Barkat, M.U. Ashraf, M. Shabbir, Feasibility of enhancing skin permeability of acyclovir through sterile topical lyophilized wafer on self-dissolving microneedle-treated skin, Dose Response 20 (2022) 15593258221097594.
[154] G. Yan, K.S. Warner, J. Zhang, S. Sharma, B.K. Gale, Evaluation needle length and density of microneedle arrays in the pretreatment of skin for transdermal drug delivery, Int. J. Pharm. 391 (2010) 7–12.
[155] B. Pamornpathomkul, T. Ngawhirunpat, I.A. Tekko, L. Vora, H.O. McCarthy, R. F. Donnelly, Dissolving polymeric microneedle arrays for enhanced site-specific acyclovir delivery, Eur. J. Pharmaceut. Sci. 121 (2018) 200–209.
[156] A.S. Aldahan, S. Mlacker, V.V. Shah, P. Kamath, M. Alsaidan, S. Samarkandy, K. Nouri, Efficacy of intralesional immunotherapy for the treatment of warts: a review of the literature, Dermatol. Ther. 29 (2016) 197–207.
[157] F.Y. Wang, Y. Chen, Y.Y. Huang, C.M. Cheng, Transdermal drug delivery systems for fighting common viral infectious diseases, Drug Deliv Transl Res 11 (2021) 1498–1508.
[158] H.S. Lee, H.R. Ryu, J.Y. Roh, J.H. Park, Bleomycin-coated microneedles for treatment of warts, Pharm. Res. (N. Y.) 34 (2017) 101–112.
[159] H.R. Ryu, H.R. Jeong, H.S. Seon-Woo, J.S. Kim, S.K. Lee, H.J. Kim, J.O. Baek, J. H. Park, J.Y. Roh, Efficacy of a bleomycin microneedle patch for the treatment of warts, Drug Deliv Transl Res 8 (2018) 273–280.
[160] M.R. Al-Naggar, A.S. Al-Adl, A.R. Rabie, M.R. Abdelkhalk, M.L. Elsaie, Intralesional bleomycin injection vs microneedling-assisted topical bleomycin spraying in treatment of plantar warts, J. Cosmet. Dermatol. 18 (2019) 124–128.
[161] J. Shan, X. Zhang, B. Kong, Y. Zhu, Z. Gu, L. Ren, Y. Zhao, Coordination polymer nanozymes-integrated colorimetric microneedle patches for intelligent wound infection management, Chem. Eng. J. 444 (2022) 136640.
[162] J. Abbasi, Microneedle sensor monitors antibiotics, JAMA 322 (2019) 1756.
[163] J. Kim, A.S. Campbell, B.E. de Ávila, J. Wang, Wearable biosensors for healthcare monitoring, Nat. Biotechnol. 37 (2019) 389–406.
[164] S. Park, Y.J. Kim, E. Kostal, V. Matylitskaya, S. Partel, W. Ryu, Highly-sensitive single-step sensing of levodopa by swellable microneedle-mounted nanogap sensors, Biosens. Bioelectron. 220 (2023) 114912.
[165] S. Bassetti, S. Tschudin-Sutter, A. Egli, M. Osthoff, Optimizing antibiotic therapies to reduce the risk of bacterial resistance, Eur. J. Intern. Med. 99 (2022) 7–12.
[166] J.A. Roberts, M.H. Abdul-Aziz, J. Lipman, J.W. Mouton, A.A. Vinks, T.W. Felton, W.W. Hope, A. Farkas, M.N. Neely, J.J. Schentag, G. Drusano, O.R. Frey, U. Theuretzbacher, J.L. Kuti, Individualised antibiotic dosing for patients who are critically ill: challenges and potential solutions, Lancet Infect. Dis. 14 (2014) 498–509.
[167] M. Dul, M. Alali, M. Ameri, M.D. Burke, C.M. Craig, B.P. Creelman, L. Dick, R. F. Donnelly, M.N. Eakins, C. Frivold, A.H. Forster, P.-A. Gilbert, S. Henke, S. Henry, D. Hunt, H. Lewis, H.I. Maibach, J.J. Mistilis, J.-H. Park, M.R. Prausnitz, D.K. Robinson, C.A.R. Hernandez, C. Ross, J. Shin, T.J. Speaker, K.M. Taylor, D. Zehrung, J.C. Birchall, C. Jarrahian, S.A. Coulman, Assessing the risk of a clinically significant infection from a Microneedle Array Patch (MAP) product, J. Contr. Release 361 (2023) 236–245.
[168] R.F. Donnelly, T.R. Singh, M.M. Tunney, D.I. Morrow, P.A. McCarron, C. O'Mahony, A.D. Woolfson, Microneedle arrays allow lower microbial penetration than hypodermic needles in vitro, Pharm. Res. (N. Y.) 26 (2009) 2513–2522.
[169] Z. Sartawi, C. Blackshields, W. Faisal, Dissolving microneedles: applications and growing therapeutic potential, J. Contr. Release 348 (2022) 186–205.
[170] M.T. McCrudden, A.Z. Alkilani, A.J. Courtenay, C.M. McCrudden, B. McCloskey, C. Walker, N. Alshraiedeh, R.E. Lutton, B.F. Gilmore, A.D. Woolfson, R. F. Donnelly, Considerations in the sterile manufacture of polymeric microneedle arrays, Drug Deliv Transl Res 5 (2015) 3–14.
[171] H.P. Swathi, V. Anusha Matadh, J. Paul Guin, S. Narasimha Murthy, P. Kanni, L. Varshney, S. Suresh, H.N. Shivakumar, Effect of gamma sterilization on the properties of microneedle array transdermal patch system, Drug Dev. Ind. Pharm. 46 (2020) 606–620.

[172] S.J. Nahas, N. Hindiyeh, D.I. Friedman, N. Elbuluk, D.J. Kellerman, P.K. Foreman, P. Schmidt, Long term safety, tolerability, and efficacy of intracutaneous zolmitriptan (M207) in the acute treatment of migraine, J. Headache Pain 22 (2021) 37.
[173] I.N. Haridass, J.C.J. Wei, Y.H. Mohammed, M.L. Crichton, C.D. Anderson, J. Henricson, W.Y. Sanchez, S.C. Meliga, J.E. Grice, H.A.E. Benson, M.A. F. Kendall, M.S. Roberts, Cellular metabolism and pore lifetime of human skin following microprojection array mediation, J. Contr. Release 306 (2019) 59–68.
[174] P.W.R. Ananda, D. Elim, H.S. Zaman, W. Muslimin, M.G.R. Tunggeng, A. D. Permana, Combination of transdermal patches and solid microneedles for improved transdermal delivery of primaquine, Int. J. Pharm. 609 (2021) 121204.
[175] A.H. Sabri, Y. Kim, M. Marlow, D.J. Scurr, J. Segal, A.K. Banga, L. Kagan, J.B. Lee, Intradermal and transdermal drug delivery using microneedles – fabrication, performance evaluation and application to lymphatic delivery, Adv. Drug Deliv. Rev. 153 (2020) 195–215.
[176] G.S. Liu, Y. Kong, Y. Wang, Y. Luo, X. Fan, X. Xie, B.R. Yang, M.X. Wu, Microneedles for transdermal diagnostics: recent advances and new horizons, Biomaterials 232 (2020) 119740.
[177] T.D. Pollard, J.J. Ong, A. Goyanes, M. Orlu, S. Gaisford, M. Elbadawi, A.W. Basit, Electrochemical biosensors: a nexus for precision medicine, Drug Discov. Today 26 (2021) 69–79.
[178] A. Keirouz, Y.L. Mustafa, J.G. Turner, E. Lay, U. Jungwirth, F. Marken, H.S. Leese, Conductive polymer-coated 3D printed microneedles: biocompatible platforms for minimally invasive biosensing interfaces, Small 19 (2023) e2206301.
[179] J. Wang, Z. Lu, R. Cai, H. Zheng, J. Yu, Y. Zhang, Z. Gu, Microneedle-based transdermal detection and sensing devices, Lab Chip 23 (2023) 869–887.
[180] H. Lee, T.K. Choi, Y.B. Lee, H.R. Cho, R. Ghaffari, L. Wang, H.J. Choi, T.D. Chung, N. Lu, T. Hyeon, S.H. Choi, D.H. Kim, A graphene-based electrochemical device with thermoresponsive microneedles for diabetes monitoring and therapy, Nat. Nanotechnol. 11 (2016) 566–572.
[181] G. Yan, K.S. Warner, J. Zhang, S. Sharma, B.K. Gale, Evaluation needle length and density of microneedle arrays in the pretreatment of skin for transdermal drug delivery, Int. J. Pharm. 391 (2010) 7–12.
[182] T. Liu, Y. Sun, G. Jiang, W. Zhang, R. Wang, L. Nie, A. Shavandi, K.E. Yunusov, U. E. Aharodnikau, S.O. Solomevich, Porcupine-inspired microneedles coupled with an adhesive back patching as dressing for accelerating diabetic wound healing, Acta Biomater. 160 (2023) 32–44.
[183] M. Zhao, M. Zhou, P. Gao, X. Zheng, W. Yu, Z. Wang, J. Li, J. Zhang, AgNPs/nGOx/Apra nanocomposites for synergistic antimicrobial therapy and scarless skin recovery, J. Mater. Chem. B 10 (2022) 1393–1402.
[184] J.A. Willis, V. Cheburkanov, S. Chen, J.M. Soares, G. Kassab, K.C. Blanco, V. S. Bagnato, P. de Figueiredo, V.V. Yakovlev, Breaking down antibiotic resistance in methicillin-resistant Staphylococcus aureus: combining antimicrobial photodynamic and antibiotic treatments, Proc. Natl. Acad. Sci. U. S. A. 119 (2022) e2208378119.
[185] X. Pang, X. Liu, Y. Cheng, C. Zhang, E. Ren, C. Liu, Y. Zhang, J. Zhu, X. Chen, G. Liu, Sono-immunotherapeutic nanocapturer to combat multidrug-resistant bacterial infections, Adv. Mater. 31 (2019) e1902530.
[186] K.R. Rouillard, O.P. Novak, A.M. Pistiolis, L. Yang, M.J.R. Ahonen, R. A. McDonald, M.H. Schoenfisch, Exogenous nitric oxide improves antibiotic susceptibility in resistant bacteria, ACS Infect. Dis. 7 (2021) 23–33.
[187] H. Lee, C. Song, Y.S. Hong, M. Kim, H.R. Cho, T. Kang, K. Shin, S.H. Choi, T. Hyeon, D.H. Kim, Wearable/disposable sweat-based glucose monitoring device with multistage transdermal drug delivery module, Sci. Adv. 3 (2017) e1601314.
[188] X. Li, X. Huang, J. Mo, H. Wang, Q. Huang, C. Yang, T. Zhang, H.J. Chen, T. Hang, F. Liu, L. Jiang, Q. Wu, H. Li, N. Hu, X. Xie, A fully integrated closed-loop system based on mesoporous microneedles-iontophoresis for diabetes treatment, Adv. Sci. 8 (2021) e2100827.
[189] X. Luo, Q. Yu, L. Yang, Y. Cui, Wearable, sensing-controlled, ultrasound-based microneedle smart system for diabetes management, ACS Sens. 8 (2023) 1710–1722.
[190] E. Schoenberg, M. O'Connor, J.V. Wang, S. Yang, N. Saedi, Microneedling and PRP for acne scars: a new tool in our arsenal, J. Cosmet. Dermatol. 19 (2020) 112–114.
[191] I.B.S. Sitohang, S.A.P. Sirait, J. Suryanegara, Microneedling in the treatment of atrophic scars: a systematic review of randomised controlled trials, Int. Wound J. 18 (2021) 577–585.
[192] M.L.B. Queiroz, S. Shanmugam, L.N.S. Santos, C.A. Campos, A.M. Santos, M. S. Batista, A.A.S. Araújo, M.R. Serafini, Microneedles as an alternative technology for transdermal drug delivery systems: a patent review, Expert Opin. Ther. Pat. 30 (2020) 433–452.